ARTICLE IN PRESS

ELSEVIER

Available online at www.sciencedirect.com
SCIENCE DIRECT®

Engineering Geology xx (2003) xxx–xxx

ENGINEERING GEOLOGY

www.elsevier.com/locate/enggeo

Site effects of the 1997 Cariaco, Venezuela earthquake

Jorge González[a,*], Michael Schmitz[a], Franck Audemard[a], Rommel Contreras[b], Antoine Mocquet[c], Jesús Delgado[d], Feliciano De Santis[a,1]

[a] *Venezuelan Foundation for Seismological Research, FUNVISIS, Apdo. Postal 76880 Caracas 1070, Venezuela*
[b] *Centro de Sismología, Universidad de Oriente, Cumaná, Venezuela*
[c] *Laboratoire de Planétologie et Géodynamique, Université de Nantes, France*
[d] *UCV-CENAMB, Caracas, Venezuela*

Received 28 April 2003; accepted 24 July 2003

Abstract

During the July 9, 1997 Cariaco earthquake, the small town of Cariaco (located 10 km SW from the epicenter) and Cumaná (capital of the State of Sucre, located about 80 km west from the epicenter) were the most affected towns. The damage in Cariaco was essentially restricted to one-century-old dwellings in the downtown area, but also three rather modern buildings collapsed. A maximum intensity of VIII (MMI) was determined for the epicentral area with a clear orientation of the major damage along the strike of the El Pilar fault in east–west direction. The induced effects associated with this event are dominated by liquefaction phenomena and lateral spreading on soft sedimentary lowlands (along the shoreline of the Cariaco Gulf and riverbeds), as well as sliding at unstable slopes. Site studies were carried out in Cariaco, involving the geotechnical analysis of boreholes, seismic refraction studies and microtremor measurements to determine the characteristics of the Quaternary sediment fill in the area. From seismic refraction surveys, an interface separating sediments with S-wave velocity lower than 700 m/s from stiffer ones was located at 60–90 m in depth in the southern part of Cariaco. Further north it is supposed to exceed 90 m. Predominant periods of soil, derived from microtremor observations in Cariaco, vary between 0.6 and 1.2 s. The high percentage of damage in the center of Cariaco can be attributed to the poor quality of the dwellings combined with the presence of thick, poorly consolidated soils, and, in some particular cases, to liquefaction phenomena.

Keywords: Cariaco earthquake; Induced effects; Site effects; Soil characteristics; S-wave velocity; Predominant periods

1. Introduction

On July 9, 1997 at 15:24 local time, an M_W 6.9 earthquake struck northeastern Venezuela (FUNVISIS, 1997), the seismically most active region in the country. The shaking was strongly felt from the eastern part of Venezuela up to the capital Caracas, located in the center of the country. Building damage was widespread in and around the town of Cariaco, where 40% of the poorly maintained "bahareque" dwellings, a traditional type of one-story adobe houses with wooden frame structure, were destroyed. Structural damage of reinforced concrete buildings occurred both in Cariaco and in the 80 km distant capital of Sucre State, Cumaná (see Fig. 1). Damage

* Corresponding author. Fax: +58-2-2579977.
E-mail address: jorgeg@funvisis.org.ve (J. González).
URL: http://www.funvisis.org.ve.
[1] Now at Ingenieros De Santis, Caracas, Venezuela.

0013-7952/$ - see front matter © 2003 Elsevier B.V. All rights reserved.
doi:10.1016/j.enggeo.2003.07.002

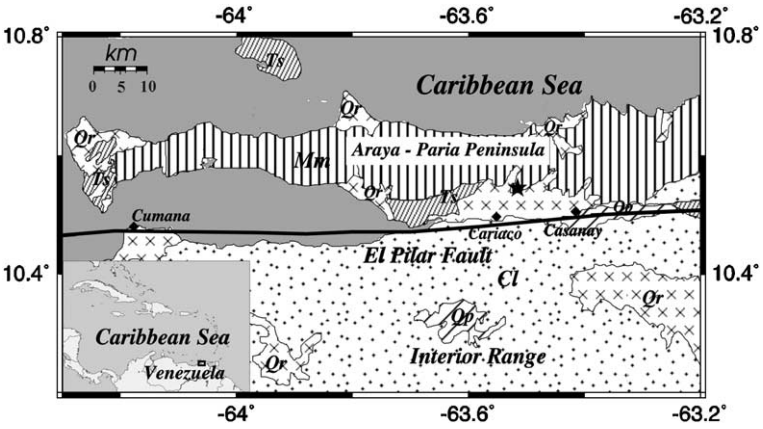

Fig. 1. Geological map of the region under study (simplified after Bellizzia et al., 1976), location of the El Pilar fault after Audemard et al. (2000). The star indicates the location of the epicenter after FUNVISIS et al. (1997), Mm = Mesozoic metamorphic rocks, Cl = Cretaceous limestones, Ts = Tertiary sediment, Qp = Quaternary sediments (Pleistocene), Qr = Quaternary sediments (recent).

resulting from induced effects was mainly concentrated on lifelines (i.e., road network and the water supply system) and some housing areas characterized by self-constructed concrete-framed masonry dwellings. No seismic-resistance considerations had been applied there, neglecting the ground conditions at riverbanks and shorelines in particular. The earthquake was the biggest event in eastern Venezuela during the 20th century, which has a remarkable record of historical earthquakes (e.g. Grases, 1990; FUNVISIS, 1994). The second most important event was the 1929 Cumaná earthquake that generated a significant amount of damage in Cumaná. A recent re-evaluation of that earthquake by Mocquet et al. (1996) questions the assigned magnitude of 6.9 because high damage that occurred during that event can be explained by the local soil conditions, which significantly amplify the effects of even moderate earthquakes. They conclude that this earthquake did not release a significant amount of stress in that region.

Both events were related to the El Pilar fault, a right-lateral strike-slip fault that belongs to a continuous fault system of some 800 km length and 100 km width in northern Venezuela. It accommodates the relative motion along the Caribbean–South American plate boundary (e.g. Minster and Jordan, 1978). Two major geological units have been recognized in the studied region: the metamorphic rocks of the Araya-Paria peninsula to the north and mainly Cretaceous sedimentary rocks of the Interior Range to the south (e.g. Metz, 1968; Vignali, 1979), both roughly separated by the El Pilar fault (Fig. 1). Neogene rocks are exposed in Cumaná, on the western edge of the Araya peninsula, northwest of Cariaco, and south of the El Pilar fault. Quaternary sediments are exposed in local basins, such as the ones where Cariaco and Cumaná are situated. The sediments that constitute the subsoil of Cariaco belong to a basin controlled by the El Pilar fault system. The basin accumulates sediments from the sedimentary range to the south and the metamorphic units to the north, which causes heterogeneity within the sedimentary fill (mainly of continental origin). Within this basin the Cariaco River left several abandoned meanders, which constitute the youngest sedimentary environment of the basin. These meanders, which are more susceptible to liquefaction phenomena, are located mainly to the south of Cariaco. Masaki et al. (1998) suggest from the evaluation of microtremor measurements that the deepest part of the sedimentary basin would be north of Cariaco. However, such a basement geometry could not be confirmed by the results of seismic studies, which indicate that the deepest part of the basin is located close to the El Pilar fault on its southern border (Schmitz et al., submitted).

In this paper, we report the results of macroseismic research, the evaluation of induced effects, and site effects in the area. Geotechnical studies, microtremor

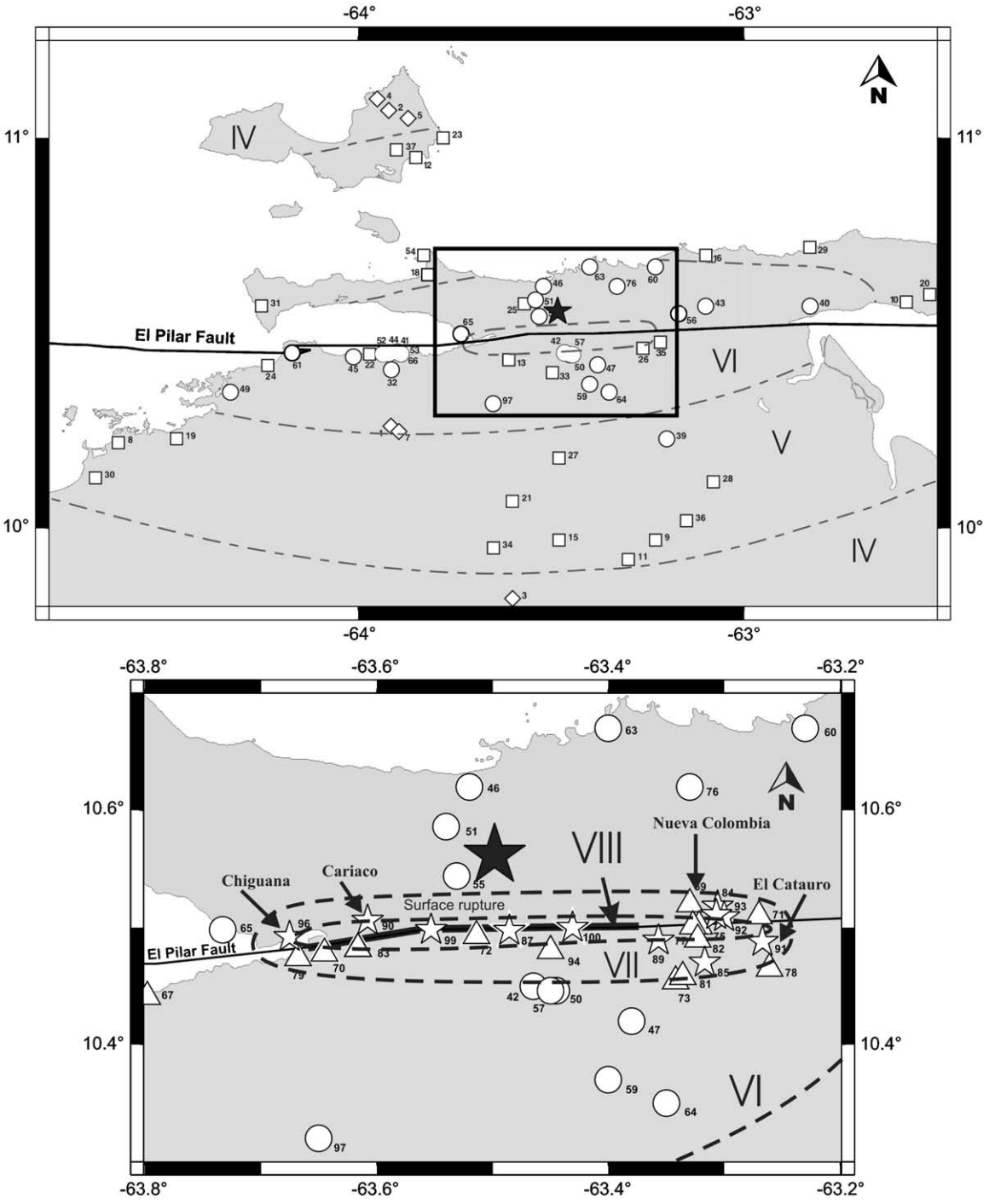

Fig. 2. The regional distribution of macroseismicity related to the 1997 Cariaco earthquake with the estimation of the MMI intensities (above) and zoom on the area related to the surface rupture (thick line; below). Observed intensities at individual data points (see Appendix A) are symbolized by rhombs: MMI = 4; squares: MMI = 5; circles: MMI = 6; triangles: MMI = 7 and stars: MMI = 8. The dark star indicates the location of the epicenter.

measurements, as well as seismic surveys were performed in order to investigate the site and induced effects in the town of Cariaco. The structural behavior of buildings, or damage is discussed in relation to specific geologic site conditions.

2. Macroseismicity studies

In order to collect Modified Mercalli Intensity Scale (MMI) data from eastern Venezuela, several field reconnaissance commissions were spread all over the region in the first 2 weeks after the earthquake. Almost 100 localities were visited and surveyed for macroseismic effects. However, the density and distribution of collected data depends on the available road network. About 300 questionnaires were analyzed for the generation of the macroseismic map, where the maximum assigned intensity is VIII (Fig. 2). Average values were determined for locations with varying values. The map integrates data collected and published by different groups (FUNVISIS, 1997; Schwarz et al., 1998; Bonato and Hernández, 1999; Mocquet and Contreras, 1999). Earthquake-related site and induced effects have not been removed from this intensity map, and are discussed in this paper.

The macroseismic map of the Cariaco 1997 earthquake (Fig. 2) clearly shows two interesting aspects:

(1) The damage is most pronounced along the El Pilar fault. The area with intensity VIII stretches over 30 km in length from Chiguana to El Cautaro, matching the extension of the surface rupturing mapped by FUNVISIS (1997) and Audemard (under review, a). However, several houses placed right on the surface rupture underwent very light or no damage at all, as reported by FUNVISIS (1997) and Audemard (1999).
(2) The damage intensity decreases with increasing distance from the epicenter, as expected, but not in the same way in all directions. Intensity attenuation is more important in north–south than in east–west direction (Fig. 3). This might indicate the existence of a strong anisotropy, or directivity effects due to the fault orientation and rupture propagation as well as by the general W–E alignment of the regional structure, whose surface expression is the regional geomorphology with a W–E oriented sedimentary (soft soil) basin and W–E striking mountain chains. In general, eastern Venezuela is characterized by major ENE–WSW trending structures (such as: folds,

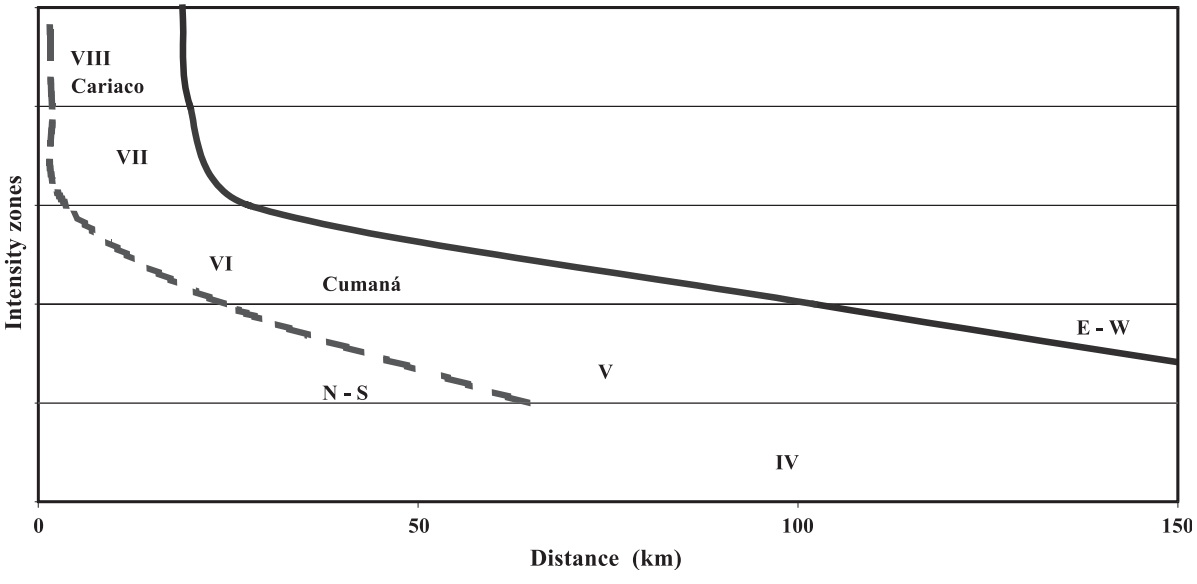

Fig. 3. Decay of macroseismic intensities in E–W direction (solid line) and N–S direction (dashed line) from epicenter. The towns of Cariaco and Cumaná show average intensities of VIII and VI, respectively.

thrusts and foliation), and east–west oriented faults, which favor energy propagation in such direction and damp it across. As a deviation from the general intensity pattern, the towns located on young alluvial plains exhibit higher levels of damage than neighboring settlements located on harder grounds.

One example is the city of Cumaná, where effects of local site conditions and induced effects occurred at a great extent (see section on induced effects in this paper; FUNVISIS, 1997; Lang et al., 1999), and intensities were higher than the average calculated for Cumaná (as displayed in Fig. 2). Cumaná has always been severely affected during most known

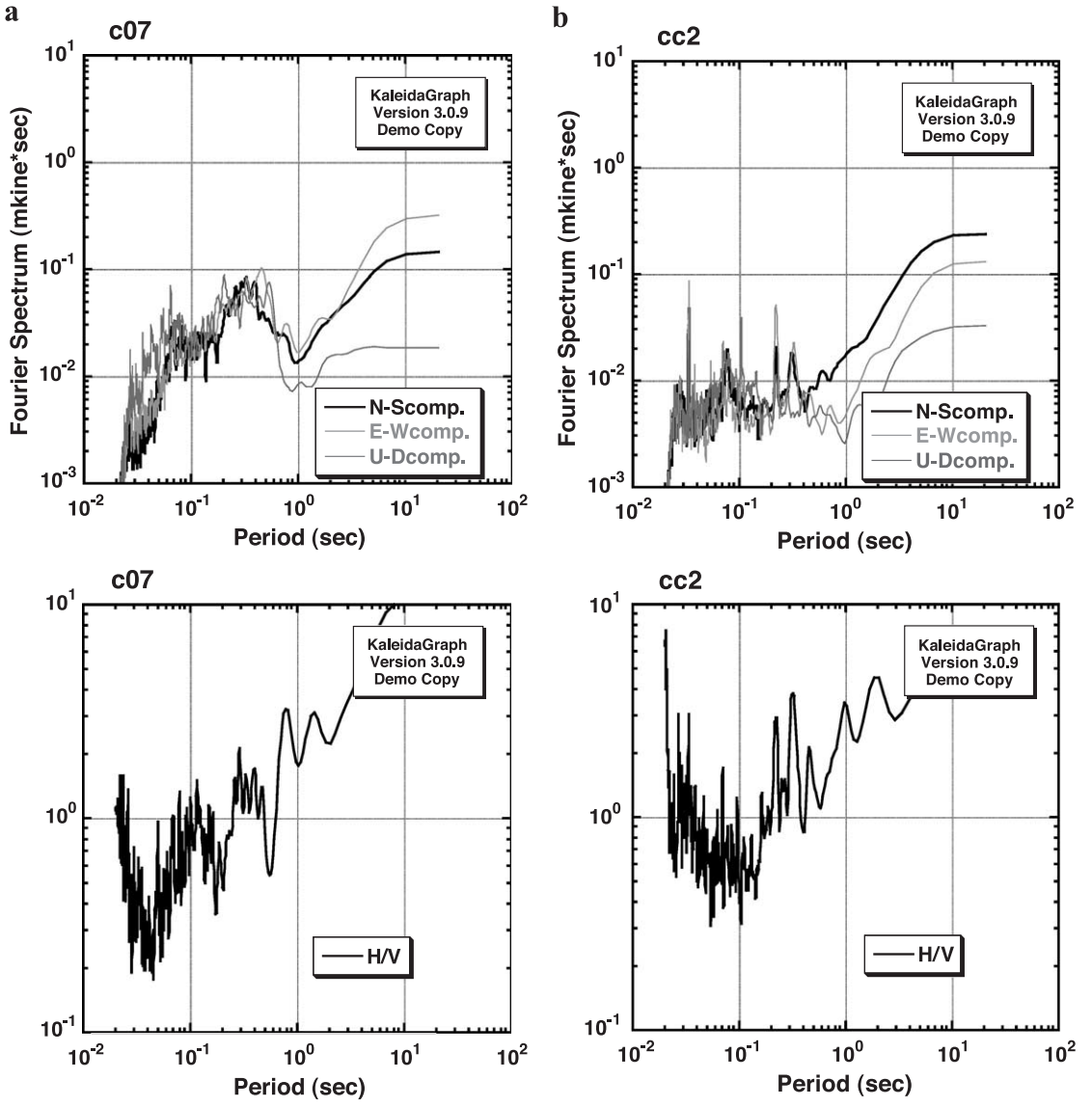

Fig. 4. Fourier spectra with the three components (above) and H/V values (below) for two sites in (a) Cariaco (c07) and (b) in the Cretaceous bedrock south of Cariaco (cc2). The site within the town (c07; for location see Fig. 5) shows a peak at 0.8 s and the bedrock site (cc2) at 0.3 s, considered as predominant periods.

earthquakes in eastern Venezuela, as attested by the repeated occurrence of induced effects, such as liquefaction and lateral spread phenomena (for further details, see Audemard, under review, b). This damage concentration can be attributed to the thick sequence of Holocene alluvial/delta plain deposits of the Manzanares River underneath the city (Beltrán and Rodríguez, 1995). Studies carried out after the Cariaco 1997

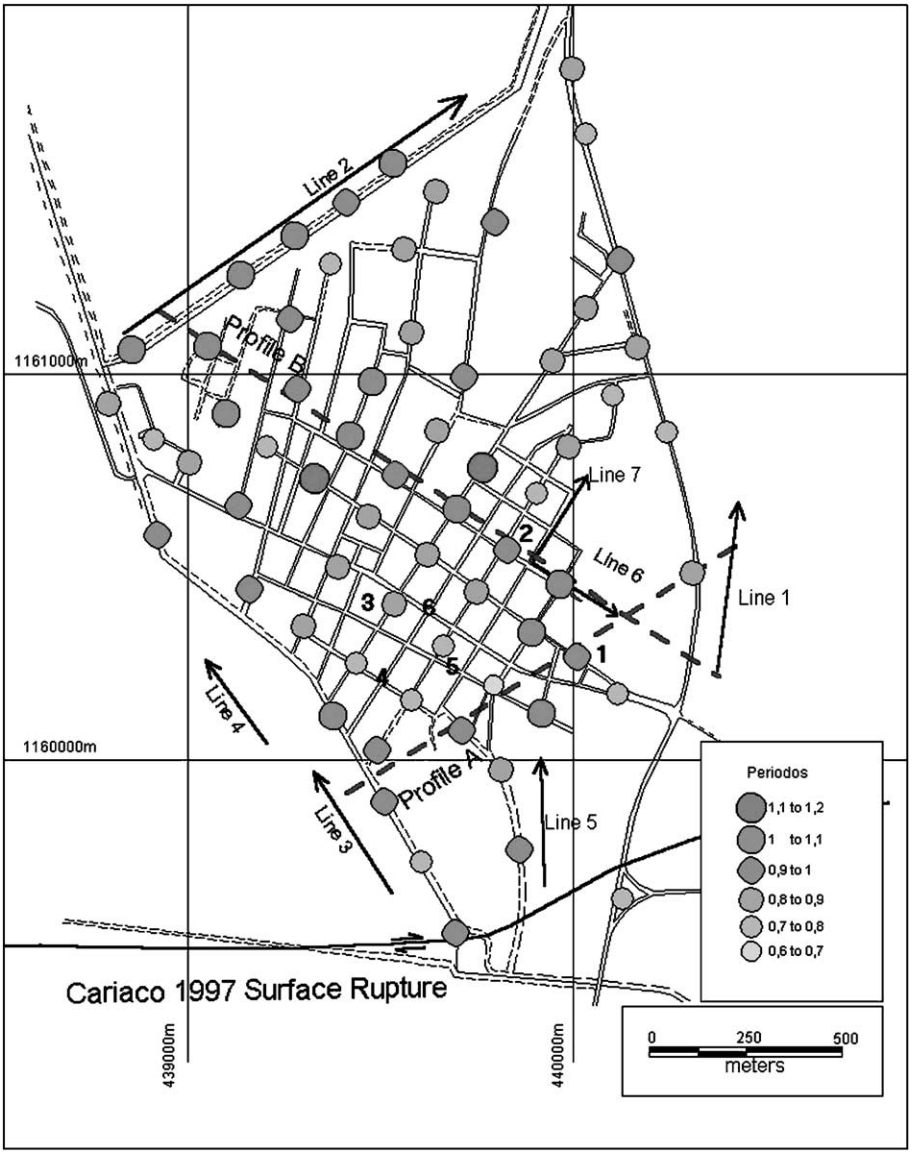

Fig. 5. Map of Cariaco with the predominant periods from microtremor measurements. The circles indicate the soil sites where measurements were performed (c07 from Fig. 4 is located northwest of line 7). The bedrock site (cc2 from Fig. 4) is located about 500 m south of the surface rupture, which separates soft soil to the north from more consolidated sediments to the south. The location of the seismic refraction lines (black lines with arrows indicating the direction of observation) as well as the composed profiles A and B (dashed lines) are indicated. 1 = Raimundo Martínez Centeno high school; 2 = Valentín Valiente school; 3 = Bank of Orinoco; 4 = Brekerman Street; 5 = Las Flores Street; 6 = Bermúdez Street.

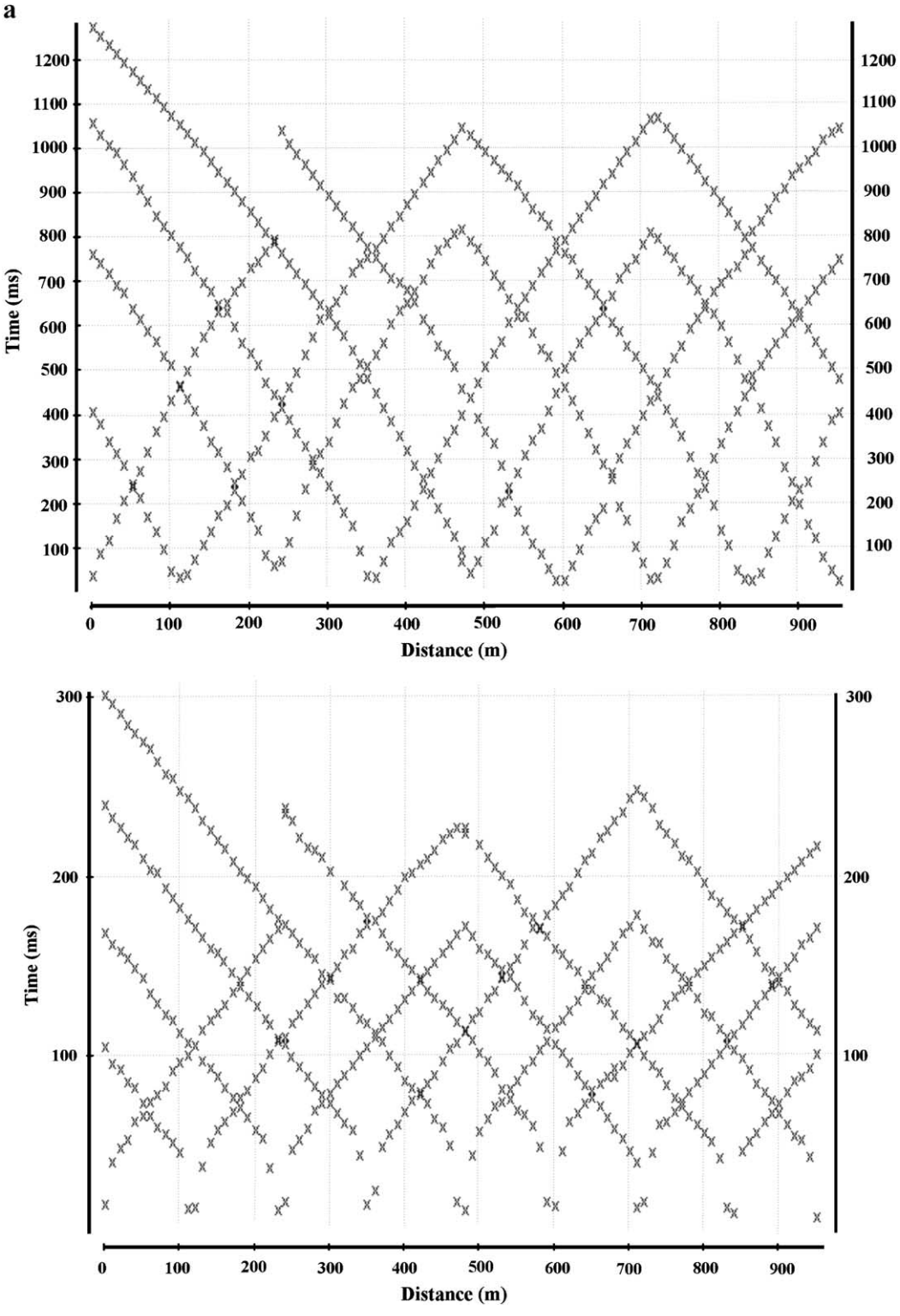
a
Time (ms)
1200
1100
1000
900
800
700
600
500
400
300
200
100
0
100
200
300
400
500
600
700
800
900
Distance (m)
Time (ms)
300
200
100
0
100
200
300
400
500
600
700
800
900
Distance (m)

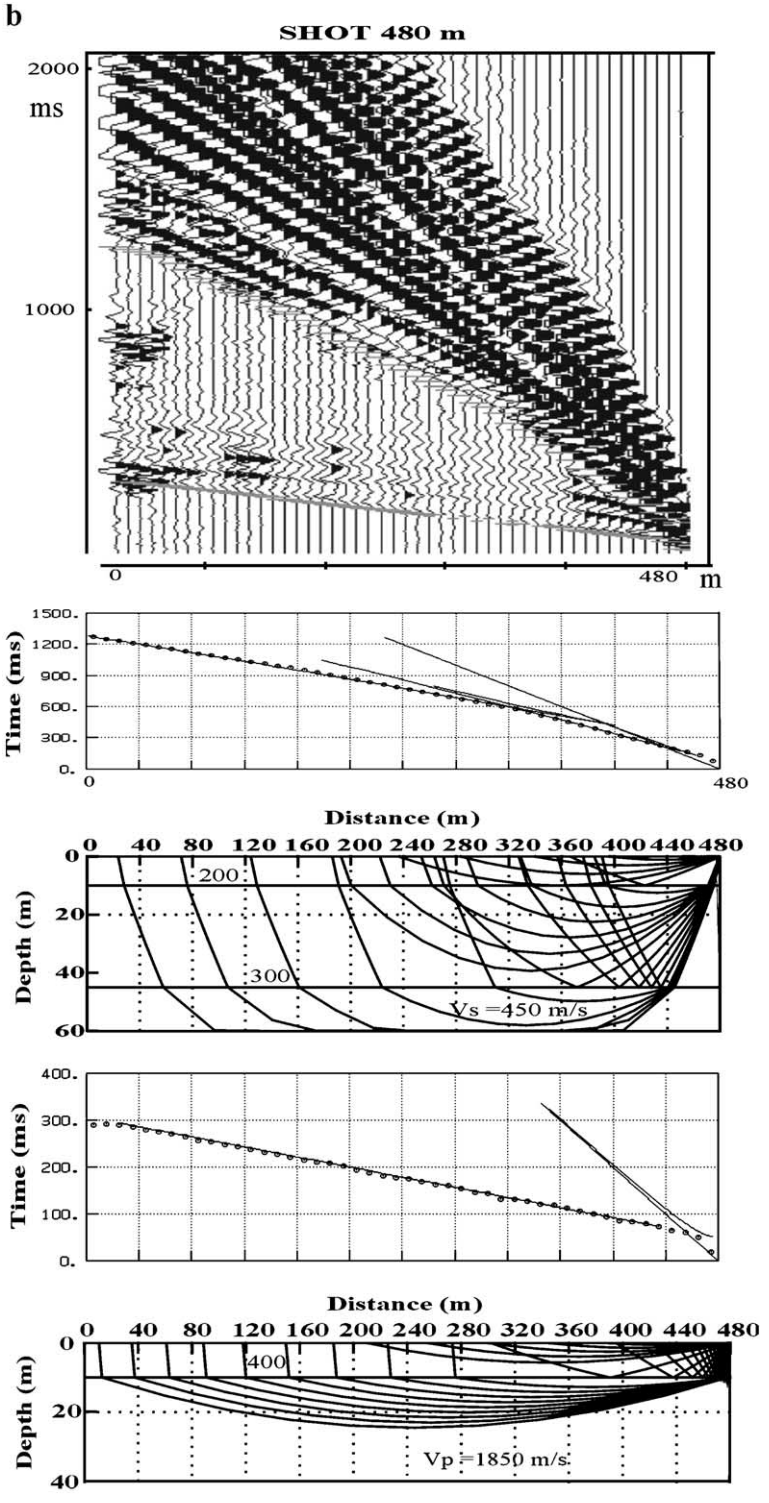
b
SHOT 480 m
2000
ms
1000
0
480
m
Time (ms)
1500.
1200.
900.
600.
300.
0.
0
480
Distance (m)
0 40 80 120 160 200 240 280 320 360 400 440 480
Depth (m)
0
20
40
60
200
300
Vs =450 m/s
Time (ms)
400.
300.
200.
100.
0.
Distance (m)
0 40 80 120 160 200 240 280 320 360 400 440 480
Depth (m)
0
20
40
400
Vp =1850 m/s

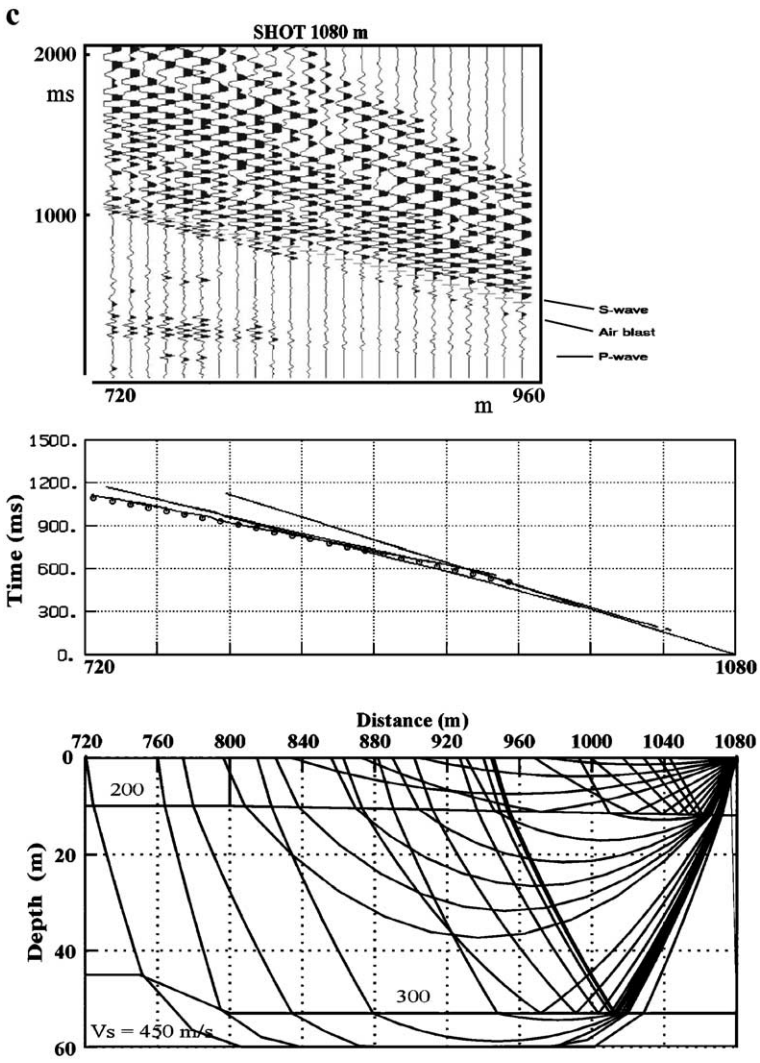

Fig. 6. Time–distance plots (a) and seismic sections (b–c) for line 2 at the northwestern border of Cariaco (for location see Fig. 5). As an example for data coverage and the control of the reciprocal times at each shot point, the picks of the first arrivals from and S-waves (above) and P-waves (below) are displayed as time–distance plots (a). Shot-point locations 480 m (b) and 1080 m (c) with the observed seismograms with picked arrivals (above), the observed (circles) and calculated (lines) travel times (center) and the calculated raypaths with the S-velocity model (below). Raypaths with velocity model and calculated P-wave travel times of shot point 480 m are displayed as well (b, lower part). First breaks of S-waves are partially overlain by signals of air blast (c).

earthquake, pointed out well the susceptibility of Cumaná to damage, among those that deserve mentioning:

(a) Microtremor analyses using the Nakamura method (Nakamura, 1989) performed by Abeki et al. (1998). They claim that the sediment sequence over large areas of the Cumaná alluvial plain is poorly consolidated since it shows long predominant periods (about 1 s) and a large H/V peak amplitude, implying the eventual occurrence of unfavorable site effects in Cumaná.
(b) Studies of soil–structure interaction (Lang et al., 1999).
(c) Estimation of the S-wave velocity at test sites in Cumaná yielding velocities as low as 250–400 m/s

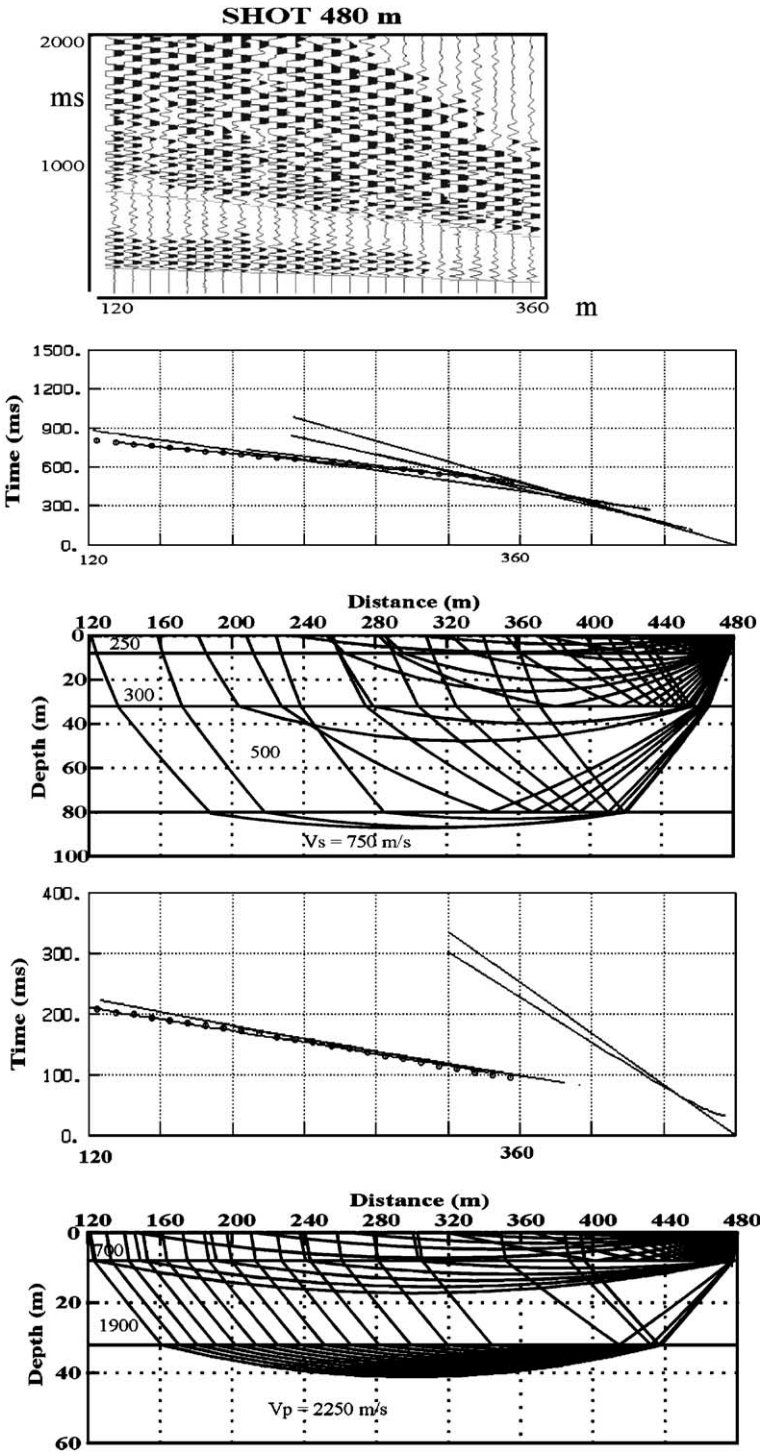

Fig. 7. Seismic section along line 3 at the southern limit of Cariaco of shot-point location 480 m with the observed seismograms with picked arrivals (above), the observed (circles) and calculated (lines) travel times (center) and the calculated raypaths with the S-velocity model (below) and the P-velocity model (lower part). No disturbance by signals of air blast is observed along this profile.

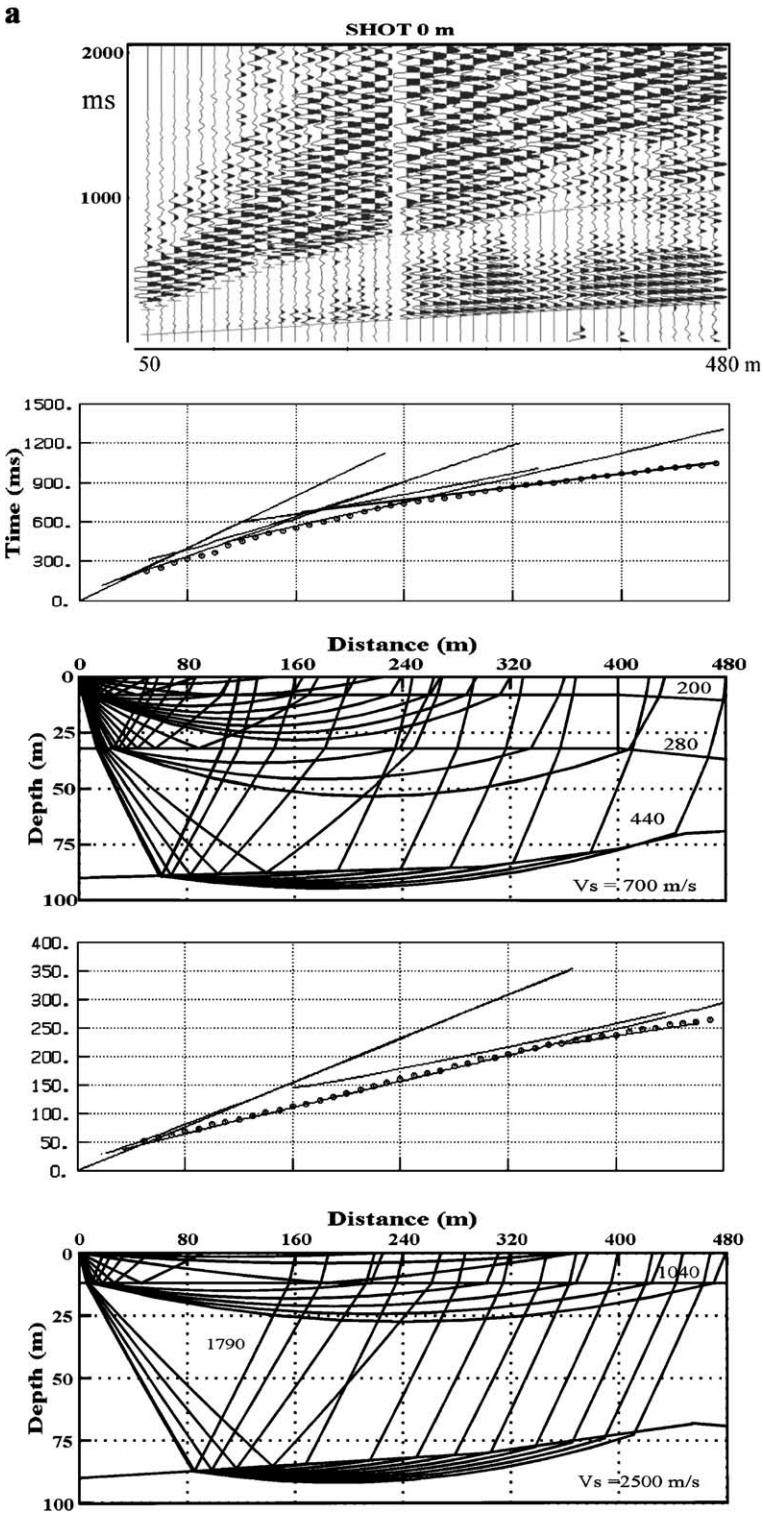
a
SHOT 0 m
2000
ms
1000
50
480 m
1500.
1200.
900.
600.
300.
0.
Time (ms)
Distance (m)
0
80
160
240
320
400
480
0
25
50
75
100
Depth (m)
200
280
440
Vs = 700 m/s
400.
350.
300.
250.
200.
150.
100.
50.
0.
Distance (m)
0
80
160
240
320
400
480
0
25
50
75
100
Depth (m)
1040
1790
Vs =2500 m/s

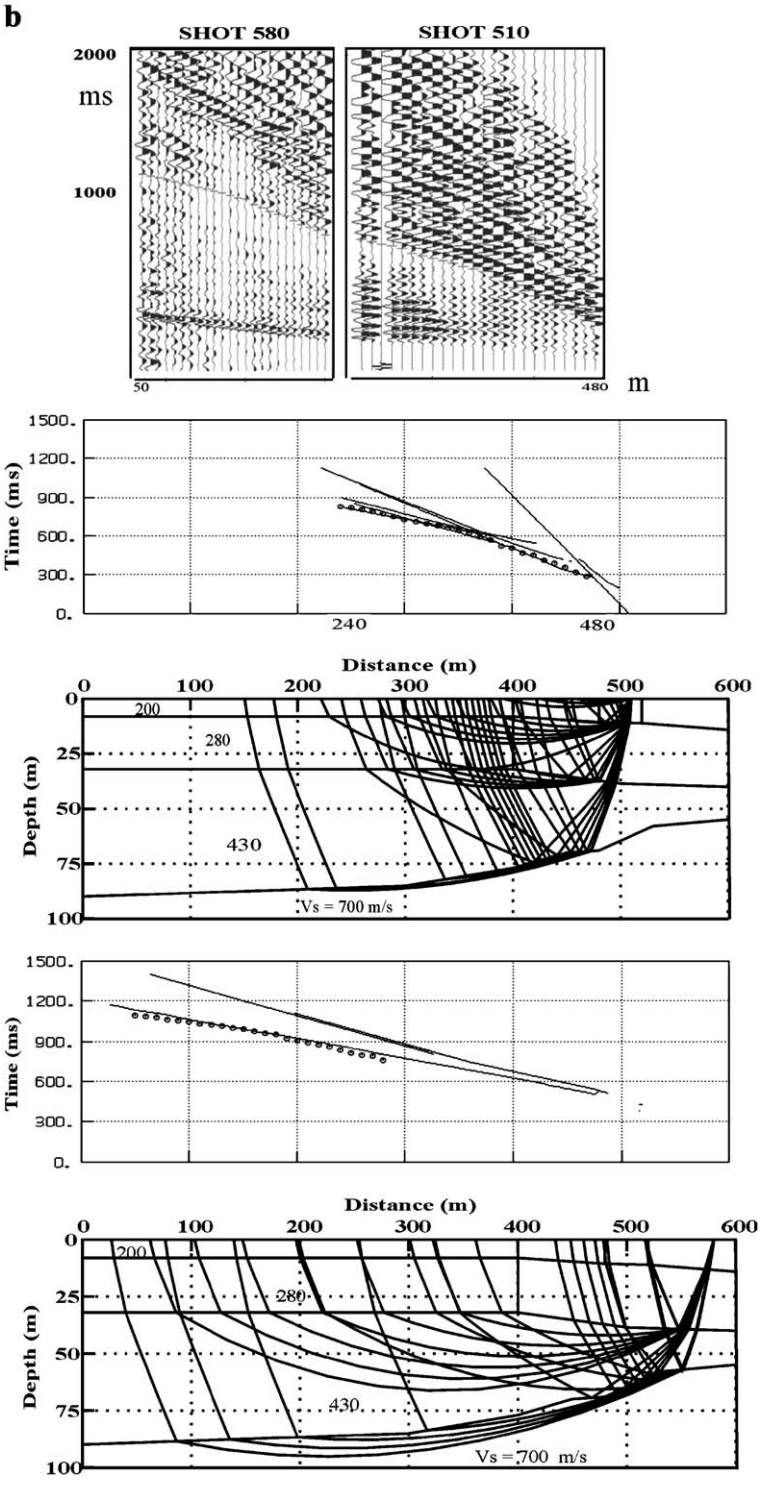
b
SHOT 580
SHOT 510
2000
ms
1000
50
480
m
Time (ms)
1500.
1200.
900.
600.
300.
0.
240
480
Distance (m)
0
100
200
300
400
500
600
Depth (m)
0
25
50
75
100
200
280
430
Vs = 700 m/s
Time (ms)
1500.
1200.
900.
600.
300.
0.
Distance (m)
0
100
200
300
400
500
600
Depth (m)
0
25
50
75
100
200
280
430
Vs = 700 m/s

for the upper 25 m of unconsolidated sediments (Kantak et al., 1999).

3. Site effects

Comprehensive geological and geophysical studies were carried out in order to characterize the soil conditions in an around Cariaco, including microtremor and seismic refraction measurements focused on the soft soils. The results of a seismic refraction study for determining the basement geometry in the town of Cariaco sedimentary basin are reported in Schmitz et al. (submitted); here, we will focus on the seismic characteristics of the soils in the town of Cariaco. The derivation of the liquefaction potential of the Cariaco subsoil was the main target of the geotechnical investigations (see Section 4.2).

3.1. Microtremor measurements

Microtremor measurements were performed at 64 sites in the Cariaco area using a broadband sensor (Guralp CMG-40T) with a natural period of 30 s and a 24-bit digitizer (Nanometrics Orion). The observation points were selected in non-noisy areas avoiding artificial noise sources. The sensors were installed on natural ground with a variable distance of 200–500 m between points. Time windows of 300 s with a sampling frequency of 100 Hz were recorded. For the calculation of the Fourier spectrum, 3000 samples (30 s) were selected at five time windows with low coherent energy from near sources and from these the H/V spectra (mean of horizontal components) were calculated following the guidelines given by Bard (1999). The characteristic peak in the H/V relation was assumed to be the predominant period of the soil site (Fig. 4).

The predominant periods within the town of Cariaco vary between 0.6 and 1.2 s (Fig. 5), whereas the bedrock sites to the south show peaks at about 0.3 s (Fig. 4b). The sites within Cariaco were divided into six groups (see Fig. 5). Slightly higher values of 0.9 to 1.1 s are observed along seismic profiles A and B, whereas lower values of 0.7 to 1.0 are observed in the northeastern part of the town of Cariaco and close to the fault rupture, but no distinct zones of equal predominant periods can be separated within Cariaco.

3.2. Seismic properties of the soils in Cariaco

The S-wave velocity of soil is among the most important geophysical parameters for the characterization and classification of a soil profile in order to determine the acceleration levels to be incorporated in the design of an earthquake-resistant structure. Therefore, seismic refraction measurements were performed in Cariaco during July 1998, also for the determination of the thickness of the soft soil, which could exhibit a strong amplification in case of an earthquake. A total of seven seismic lines were recorded in Cariaco (Fig. 5). The individual seismic line lengths varied between 360 and 1080 m with maximum shot-receiver offsets between 120 and 480 m; the geophone spacing varied between 5 and 10 m for the different lines. The shots were located at both ends and in the center (along line 2 shot points were located each 120 m). Pentolite charges between 100 and 400 g at a depth of 0.5 to 1 m were used as energy source. A 24 channel Geometrics StrataView seismic recorder and 14 Hz geophones were employed. The data were processed and analyzed using the REFRA seismic refraction software (Sandmeier, 1998) for identifying first breaks. 1-D models were calculated using the intercept–time method (e.g. Palmer, 1986), including the control of reciprocal times (Fig. 6a). Forward modeling based on the results of the 1-D models was applied along each seismic line using the 2-D raytracing RAYAMP program (Crossley, personal communication).

The analysis of the first breaks of the P-waves indicates that the velocity of the uppermost layer varies between 400 and 1040 m/s and the depth between 4 and 14 m. Below, the velocity of the saturated sediments ranges between 1700 and 1900 m/s (Figs. 6–8;

Fig. 8. Seismic sections along line 1 at the eastern limit of Cariaco of shot-point locations 0 m (a) and 510/580 m (b) with the observed seismograms with picked arrivals (above), the observed (circles) and calculated (lines) travel times (center) and the calculated raypaths with the S-velocity model (below). Raypaths with velocity model and calculated P-wave travel times of shot point 0 m are displayed as well (a, lower part). A deeper high velocity layer, which is inclined towards the north, is observed in the S-waves (700 m/s) as well as in the P-waves (2500 m/s). The geometry of the top of the deeper layer is well confirmed by the two shot points at 510 and 580 m (b).

Table 1). On line 3, we identified a third layer at 32 m depth with Vp = 2250 m/s, and along line 1, an increase to P-wave velocities of 2500 m/s is observed between 60 and 90 m in depth (Fig. 8a). For identifying the layering inside the saturated zone we used the S-waves. A problem for the recognition of the S-wave first breaks is the superposition with the air blast arrival (Fig. 6c). Generally, arrivals from the air blast precede the S-wave arrivals some 0–100 ms and make the recognition of later phases difficult. Despite the existence of the air blast energy in some sections, data quality is good and picks of first breaks can be done with good accuracy. The arrivals of the S-waves cannot be unambigously distinguished from possible arrivals of surface waves. Nevertheless, the difference in seismic velocity (the velocity of the Rayleigh wave is 0.919 times the velocity of the S-waves; Sheriff and Geldart, 1995) between both wave-types would result in only slightly elevated S-wave velocities, if Rayleigh waves were picked.

Table 1
P-wave and S-wave velocities for the seismic lines in Cariaco (for location see Fig. 5)

	Depth (m)	Vp (m/s)	Vs (m/s)
Line 1	0–8/14	1040	200
	8/14–32/40	1790	280
	32/40–60/90	1790	430
	60/90–	2500	700
Line 2	0–10	500	200/250
	10–45/53	1750	300
	45/53–	–	450
Line 3	0–8	700	250
	8–32	1900	300
	32–80	2250	500
	80–	–	750
Line 4	0–7/10	800	200
	7/10–35/38	1730	320
	35/38–	–	440
Line 5	0–4/12	700	200
	4/12–30/60	1800	320/350
	30/60–	–	450/500
Line 6	0–4	600	150
	4–12	600	250
	12–40	1700	300
	40–90	–	450
	90	–	680
Line 7	0–10	700	200
	10–45	1700	300
	45–	–	420

Generally, two strata are displayed for P-wave velocities, the unsaturated sands and clays (400–1040 m/s) in the upper 4–14 m and the water-saturated sediments (1700–1900 m/s) below. The groundwater level (top of the second layer) is quite deep compared to the observations right after the earthquake (see Section 4.2), which is attributed to the dry weather conditions during seismic measurements. From the evaluation of P-velocities, deeper layers are only detected on lines 3 and 1 with velocities of 2250 and 2500 m/s, respectively, the latter one interpreted as base of the Quaternary sediments. The distribution of S-wave velocities is displayed in Fig. 9.

Along line 2 at the northwestern limit of Cariaco (Fig. 6), an upper layer with an S-wave velocity of 200–250 m/s overlays one with a velocity of 300 m/s. The boundary is located at a depth of 10 m. Below that depth, a velocity increase to 450 m/s is observed with the depth increasing from 45 to 53 m towards the NE. Arrivals from deeper layers cannot be observed along this line, although the data is of good quality throughout the seismic section up to the maximum recording distance of 480 m. On other seismic sections, high velocity layers (700–750 m/s) at depths of about 80–90 m appear at an offset of 250–350 m (Figs. 7 and 8a). Therefore, we can infer that the depth of a layer with a velocity significantly higher than 450 m/s should exceed 90 m on line 2 (Fig. 9). At the southern border of Cariaco (line 3, Fig. 7), the increase to 750 m/s is observed at a depth of 80 m, whereas at the eastern border (line 1, Fig. 8), the interface with an S-wave velocity of 700 m/s is dipping from north (60 m) to south (90 m). This dipping is well constrained by the observations at shot points 580 and 510 (Fig. 8b). The same interface can be derived from P-wave data and the underlaying layer has a velocity of 2500 m/s. Along line 5, which is located further south and therefore closer to the El Pilar fault, lateral variations are observed with a decrease of the top of the layer with 500 m/s to 60 m in depth at the southern end.

This velocity information of the Cariaco subsoil was summarized in profiles A and B trending SW–NE and NW–SE, respectively (Fig. 9), roughly corresponding to the shorter and longer dimensions of the town. Along profile A, which correlates across seismic lines 3, 5 (projected), 6 and 1 (northern end of this line), the velocities in the first three layers decrease slightly towards northeast and the top of the 700 m/s layer decreases in depth in the same direction from 90 to 60 m in depth. This layer is interpreted either as the weathered top of the Creta-

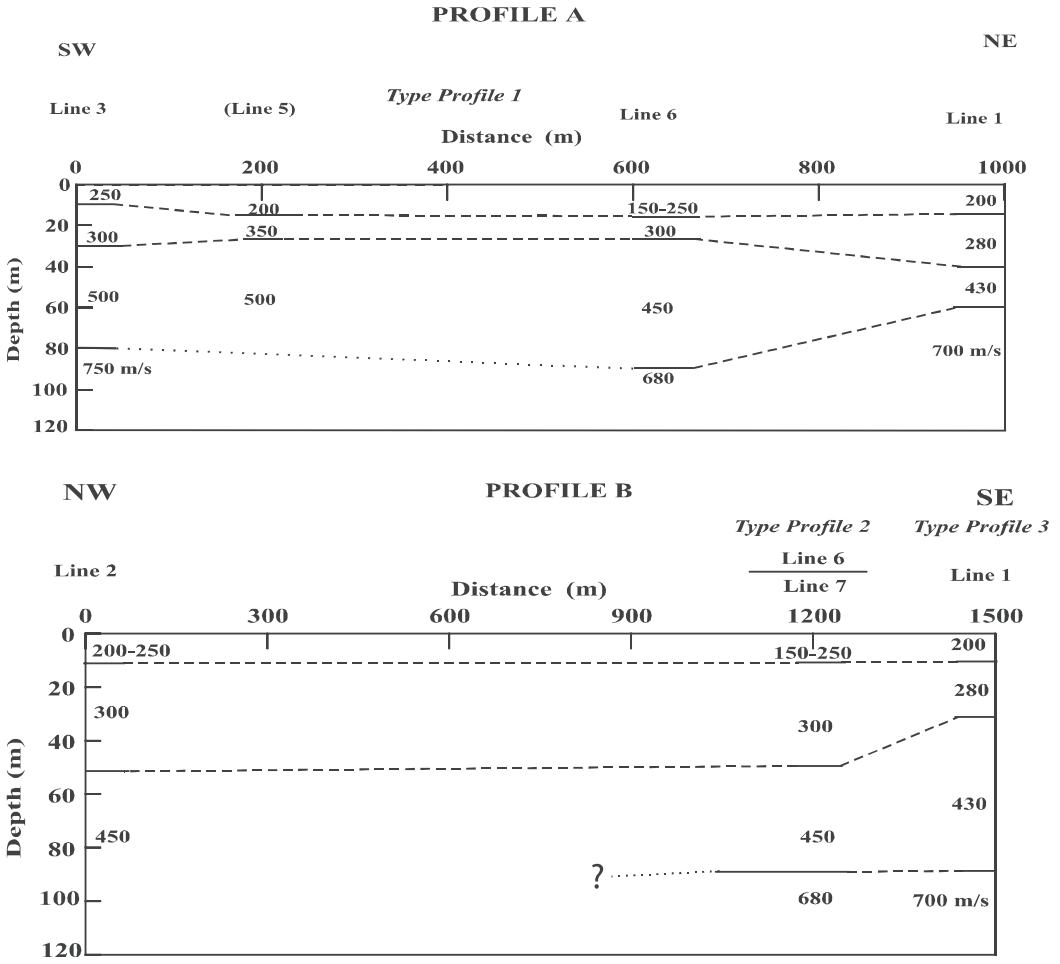

Fig. 9. Composed profiles A (top) and B (bottom) located at the southeastern border and in the northwestern part of Cariaco, respectively. The numbers represent the S-wave velocities for each layer. Solid lines: measured, dashed lines: interpolation. The type profiles indicate the locations for which response spectra (Fig. 10) were calculated. For location, see Fig. 5; vertical exaggeration for profile A, 3:1; for profile B, 6:1.

ceous limestones exposed on the southern flank of the Cariaco sedimentary valley, or as Tertiary sediments exposed some 5 km west of Cariaco (Fig. 1). The intermediate layer with an S-velocity between 440 and 520 m/s might correspond to coarse grained sand with gravel deposited from the south, whereas the uppermost layers with low seismic velocity are interpreted as fine sand interbedded with clay.

Profile B, which is crossing Cariaco from NW to SE, displays the information from lines 2, 6, 7 and 1 (southern end of this line). Here, an increase in thickness of material with low seismic velocities towards the center of the basin in the north can be observed (Fig. 9b). The deepest layer with an S-velocity of 680–700 m/s is only observed on lines 1 and 6 (SE portion of profile B), at a depth of about 90 m. This layer could not be detected along line 2. Therefore, we can assume an increase in depth towards the north. If we regard the top of this layer as the limit of the Quaternary sedimentary infill of the basin, the total thickness of the Quaternary sediments in Cariaco exceeds 90 m.

3.3. Importance of local site conditions during the Cariaco 1997 earthquake to damage

Soil conditions determine the dynamic characteristics of a site, meaning that strong variations in

seismic response and damage distribution can be observed between nearby sites, as evidenced for example during the 1967 Caracas earthquake (Seed et al., 1970). A strong correlation between surface geology and damage distribution has been observed for damaging earthquakes, especially in areas with unconsolidated sediments (Rosenblueth and Ovando, 1991). For engineering purpose, unconsolidated sediments (or "soft soil") with S-wave velocities below 700 m/s are discriminated from consolidated sediments or bedrock ("hard soils") with higher velocities (e.g. Seed et al., 1990). The new seismic building code in Venezuela (COVENIN, 2001) refers to the S-wave velocity as an important parameter for the characterization of the soil profile. In this context, civil engineers use the term soils interchangeably with terms like sediments and fill, referring to any deposit, such as clays, sands, silts, or gravel above bedrock.

The most severe structural damages on reinforced concrete buildings occurred in the city of Cumaná and in the town of Cariaco. In Cumaná, the Miramar, a seven floor reinforced concrete building, collapsed because of design problems such as the irregular distribution of rigidities and the inappropriate structural design of the traverse steel elements (Bonilla et al., 2000).

In Cariaco, the Valentín Valiente School, built in 1958, had a reinforced concrete structure of two levels with a rectangular plan, with frames only across. Big horizontal displacements in the longer direction caused the partial collapse of this structure. The U-shaped building of the Raimundo Martínez Centeno high school, built in 1989, was composed of two 3-level structures. The collapse of the first level of the two main blocks occurred due to the inadequate distribution of the masonry brick walls and big horizontal displacements at the foundation level. The Cariaco branch of the Bank of Orinoco was a two-story structure, the first level of reinforced concrete and the second level of steel beams. In this case, the second level collapsed completely upon the first one. This structure had been built in two parts without an appropriate connection between the original structure and the extension (Bonilla et al., 2000).

No distinct zones of equal predominant period can be distinguished in Cariaco (Fig. 5), but a general trend indicates lower values close to the fault rupture, e.g. the southeastern limit of the sedimentary basin, increasing towards NW. Most of the calculated predominant periods within Cariaco are in a relatively close range between 0.8 and 1.0 s, which corresponds roughly to a thickness in the order of some 70 to 110 m (considering the average velocities varying between 280 and 350 m/s and applying the simple relation of period equals average velocity divided by four times the thickness), which coincides well with the thickness of the unconsolidated sediments as derived from the seismic measurements. No direct correlation can be done between the results of the microtremor measurements and the seismic refraction measurements (Figs. 5 and 9), as the variations of the predominant periods within the observed range are stronger than the corresponding changes in the S-wave velocities and thickness of unconsolidated sediments. Nevertheless, the locations of the collapsed reinforced concrete buildings (numbers 1–3 in Fig. 5) and the damage concentrated between the Brekerman and Bermúdez streets (4–6 in Fig. 5) coincide with predominant periods of around 1 and 0.7 s, respectively.

Based on the seismic velocities, the response spectra for three type-profiles in Cariaco (Table 2, see Fig. 9 for location) were calculated (Fig. 10). As no strong motion data were available from the Cariaco area, an accelerogram from the 1979 Imperial Valley at 10.6 km distance to the rupture was used as input. This earthquake had a similar magnitude (Ms 6.9) and rupture mechanism (dextral strike-slip) compared to the Cariaco 1997 earthquake, and the epicentral distances match as well.

No disturbance is observed at periods below 0.1 s at the surface (Fig. 10). In general, energy is absorbed by the sediments to about 0.4 s, and amplification occurs between 0.4 and 3 s for type-profiles 1 and 3, and between 0.8 and 3 s for type-profile 2. For all three soil profiles the acceleration values exceed 0.5 g, and reaches 0.8 g between 0.4 and 0.7 s for type-profiles 1 and 3, although type-profile 3 has a smaller soil thickness. The range between 0.4 and 0.7 s with the highest values of acceleration do not coincide well with the predominant periods from microtremor measurements (Fig. 5). Therefore, we do not consider the amplification effects as the main cause for the damage that occurred in Cariaco during the 1997 event.

Table 2
Input data of the Proshake 1.1 program (based on Schnabel et al., 1972) for the dynamic response evaluation of type-profiles 1, 2 and 3 (Fig. 10)

Layer number	Material name	Thickness (m)	Unit weight (pcf)	Gmax (ksf)	Vs (m/s)	Modulus curve	Damping curve
Type-profile 1, water table: 5 m; number of layers: 12							
1	Clay (CL) IP = 16	5.00	99.88	1336.66	200.00	Clay-PI = 10–20 (Sun et al.)	Clay-average (Sun et al.)
2	Clay (CL) IP = 20	5.00	99.88	1336.66	200.00	Clay-PI = 20–40 (Sun et al.)	Clay-upper bound (Sun et al.)
3	Clay (CL) IP = 30	5.00	106.1	3195.48	300.00	Clay-PI = 20–40 (Sun et al.)	Clay-upper bound (Sun et al.)
4	Sand (SG)	5.00	106.1	3195.48	300.00	Sand (Seed and Idriss)-average	Sand (Seed and Idriss)-average
5	Sand (SG)	10.00	106.1	3195.48	300.00	Sand (Seed and Idriss)-average	Sand (Seed and Idriss)-average
6		10.00	112.37	8661.59	480.00	Sand (Seed and Idriss)-average	Sand (Seed and Idriss)-average
7		10.00	112.37	8661.59	480.00	Sand (Seed and Idriss)-average	Sand (Seed and Idriss)-average
8		10.00	112.37	8661.59	480.00	Sand (Seed and Idriss)-average	Sand (Seed and Idriss)-average
9		10.00	112.37	8661.59	480.00	Sand (Seed and Idriss)-average	Sand (Seed and Idriss)-average
10		10.00	112.37	8661.59	480.00	Sand (Seed and Idriss)-average	Sand (Seed and Idriss)-average
11		10.00	118.61	18,348.65	680.00	Sand (Seed and Idriss)-upper bound	Sand (Seed and Idriss)-upper bound
12	Rock equivalent	Infinite	118.61	18,348.65	680.00	Rock	Rock
Type-profile 2, water table: 5 m; number of layers: 12							
1	Clay (CL) IP = 20	5.00	99.88	1336.66	200.00	Clay-PI = 10–20 (Sun et al.)	Clay-average (Sun et al.)
2	Clay (CL) IP = 20	5.00	99.88	1336.66	200.00	Clay-PI = 10–20 (Sun et al.)	Clay-upper bound (Sun et al.)
3	Clay (CL) IP = 20	5.00	106.13	3195.48	300.00	Clay-PI = 10–20 (Sun et al.)	Clay-upper bound (Sun et al.)
4	Sand (SM)	5.00	106.13	3195.48	300.00	Sand (Seed and Idriss)-average	Sand (Seed and Idriss)-average
5	Sand (SM)	10.00	106.13	3195.48	300.00	Sand (Seed and Idriss)-average	Sand (Seed and Idriss)-average
6		10.00	106.13	3195.48	300.00	Sand (Seed and Idriss)-average	Sand (Seed and Idriss)-average
7		10.00	106.13	3383.44	300.00	Sand (Seed and Idriss)-average	Sand (Seed and Idriss)-average
8		10.00	112.37	7612.73	450.00	Sand (Seed and Idriss)-average	Sand (Seed and Idriss)-average
9		10.00	112.37	7612.73	450.00	Sand (Seed and Idriss)-average	Sand (Seed and Idriss)-average
10		10.00	112.37	7612.73	450.00	Sand (Seed and Idriss)-average	Sand (Seed and Idriss)-average
11		10.00	112.37	7612.73	450.00	Sand (Seed and Idriss)-upper bound	Sand (Seed and Idriss)-upper bound
12	Rock equivalent	Infinite	118.61	18,348.65	680.00	Rock	Rock
Type-profile 3, water table: 5 m; number of layers: 12							
1	Clay (CL) IP = 20	5.00	106.13	1420.21	200.00	Clay-PI = 10–20 (Sun et al.)	Clay-average (Sun et al.)
2	Clay (CL) IP = 20	5.00	106.13	1420.21	200.00	Clay-PI = 10–20 (Sun et al.)	Clay-upper bound (Sun et al.)
3	Clay (CL) IP = 20	5.00	106.13	2783.61	300.00	Clay-PI = 10–20 (Sun et al.)	Clay-upper bound (Sun et al.)
4	Sand (SM)	10.00	106.13	2783.61	300.00	Sand (Seed and Idriss)-average	Sand (Seed and Idriss)-average
5	Sand (SM)	10.00	106.13	2783.61	300.00	Sand (Seed and Idriss)-average	Sand (Seed and Idriss)-average
6		10.00	106.13	2783.61	300.00	Sand (Seed and Idriss)-average	Sand (Seed and Idriss)-average
7		10.00	112.37	6951.08	430.00	Sand (Seed and Idriss)-average	Sand (Seed and Idriss)-average
8		10.00	112.37	6951.08	430.00	Sand (Seed and Idriss)-average	Sand (Seed and Idriss)-average
9		10.00	112.37	6951.08	430.00	Sand (Seed and Idriss)-average	Sand (Seed and Idriss)-average
10		10.00	118.60	7336.46	430.00	Sand (Seed and Idriss)-average	Sand (Seed and Idriss)-average
11		32.81	118.60	19,442.22	700.00	Sand (Seed and Idriss)-upper bound	Sand (Seed and Idriss)-upper bound
12	Rock equivalent	Infinite	118.61	19,443.86	700.00	Rock	Rock

Input data consider the geotechnical characteristics (Section 4.2) as well as S-wave velocities (Fig. 9). The shear module Gmax was calculated based on the curves of Vucetic and Dobry (1991). Modulus and damping curves for clay after Sun et al. (1988) and for sand after Seed and Idriss (1970).

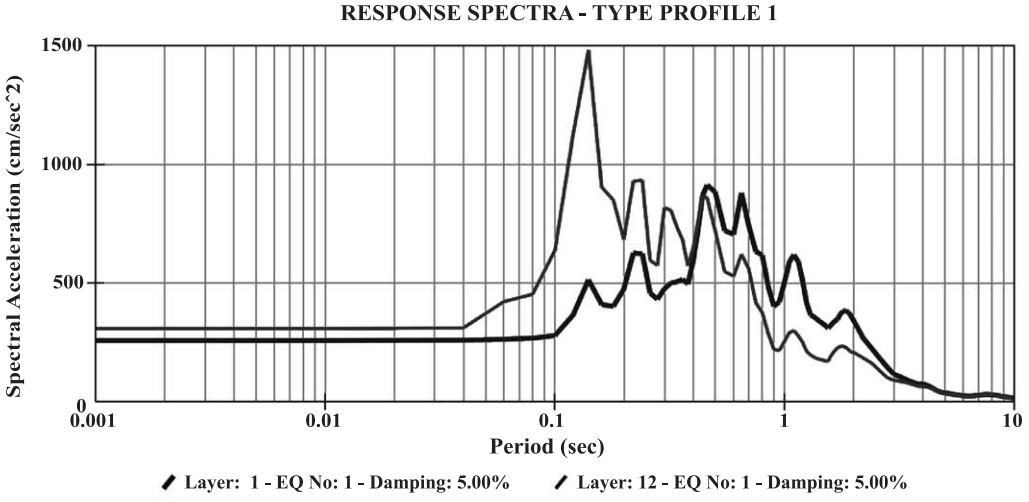
RESPONSE SPECTRA - TYPE PROFILE 1
Spectral Acceleration (cm/sec^2)
1500
1000
500
0
0.001
0.01
0.1
1
10
Period (sec)
Layer: 1 - EQ No: 1 - Damping: 5.00%
Layer: 12 - EQ No: 1 - Damping: 5.00%

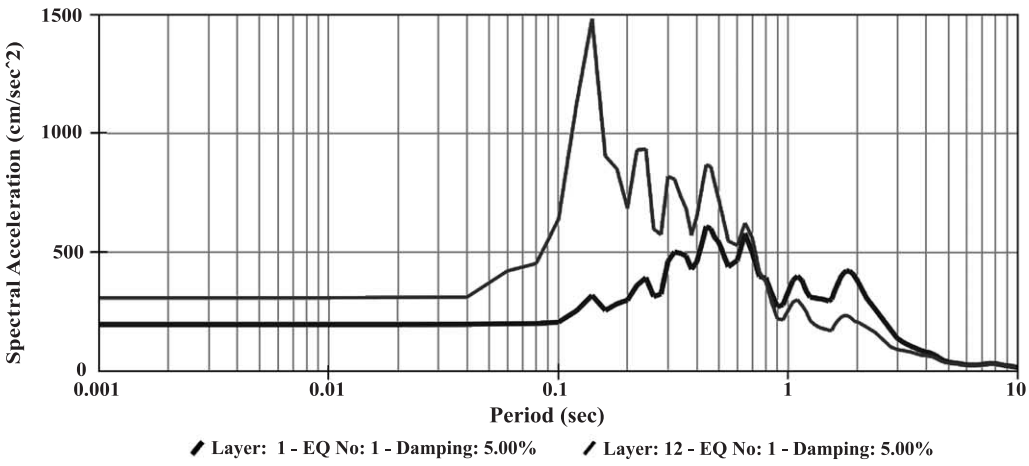
RESPONSE SPECTRA - TYPE PROFILE 2
Spectral Acceleration (cm/sec^2)
1500
1000
500
0
0.001
0.01
0.1
1
10
Period (sec)
Layer: 1 - EQ No: 1 - Damping: 5.00%
Layer: 12 - EQ No: 1 - Damping: 5.00%

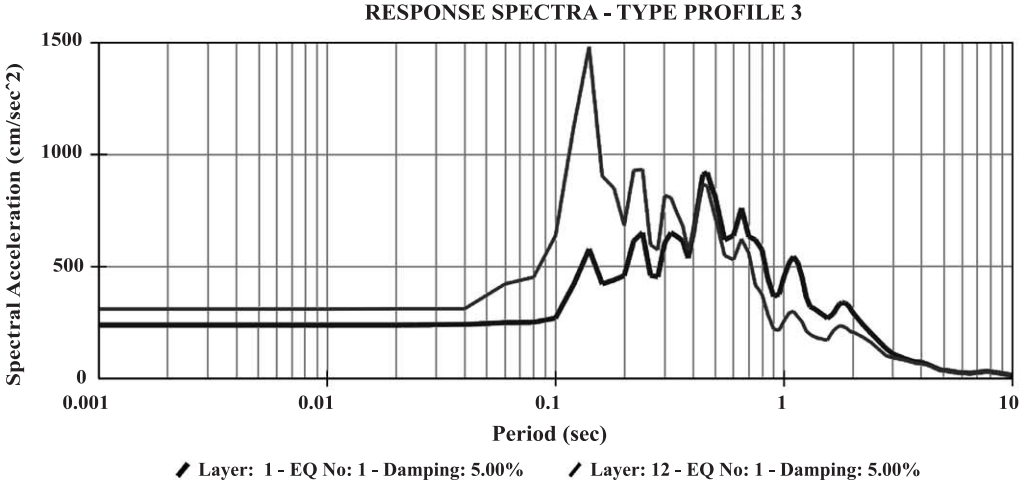
RESPONSE SPECTRA - TYPE PROFILE 3
Spectral Acceleration (cm/sec^2)
1500
1000
500
0
0.001
0.01
0.1
1
10
Period (sec)
Layer: 1 - EQ No: 1 - Damping: 5.00%
Layer: 12 - EQ No: 1 - Damping: 5.00%

4. Induced effects by the Cariaco earthquake

Induced effects associated with the Cariaco 1997 earthquake were very common and widespread because conditions were given for either mass instabilities in areas of rough/unstable topography or liquefaction and lateral spread in low-lying young alluvial plains (Fig. 11). The epicentral region is located on a poorly drained Holocene alluvial plain (the Cariaco sedimentary basin with the Campoma and Buena Vista swamps) at the eastern end of the Cariaco Gulf. This plain is bounded to the south by the Interior range, comprising Cretaceous sedimentary rocks (Fig. 1), reaching a height of more than 1000 m over less than 10 km (10% gradient). Further west the range falls abruptly down into the Cariaco Gulf where the existing flatlands along its coasts mainly correspond to active Holocene alluvial/delta plains growing at the major river mouths. To the west, induced effects have been reported as far as the western seashore of Cumaná (Fig. 12), some 80 km west of the epicenter. But to the east, these effects are observed only up to the surrounds of Nueva Colombia, about 25 km away from the epicenter. Only few induced effects were observed on the northern coast of the Cariaco Gulf and at the northern limit of the Cariaco sedimentary basin (Fig. 11). Here, topography is much smoother and the bedrock consists mainly of Mesozoic metamorphic rocks (Fig. 1).

4.1. Liquefaction and lateral spreading

Most frequent liquefaction features reported in association with the Cariaco 1997 earthquake are sand blows, and occasionally sand-vent fractures, but this latter ones are generally related to lateral spreading (Plate 1A and B). However, not all lateral spreads did show venting. At the Piragua pool (north of Aguas Calientes, on the southern limit of the Buena Vista swamp), a northward lateral spreading towards a very shallow creek unequivocally destroyed ground surface though any sand venting occurred (Plate 1C and D). The evidence to support this interpretation are the following concurrent features: curved shape of wide-open tension cracks affecting a rather flat topography; considerable amount of opening across the cracks indicates that some translation happened; tilting of tops of slabs bounded by tension cracks also denotes some rotation; the presence of a shallow (about 0.5 m deep) water table; and topmost sedimentary sequence observed in crack walls comprises a thick sandy layer.

Sand blows were observed between Laguna de Buena Vista in the east and the eastern coast of Cumaná at Punta Baja (north of El Peñon) to the west (Figs. 11 and 12). All reported liquefaction features are in active alluvial plains around the Cariaco Gulf. Besides the evidence in the Buena Vista-Campona region, the remaining sites exhibiting liquefaction correspond to Holocene delta plains along the seashore of the Cariaco Gulf and seldomly to sandy beaches, such as Tocuchare and Ensenada Honda (Fig. 11A). At the latter place, locals reported white sand venting along an east–west trending fracture below the intertidal zone, as aligned sand blows, when sea receded several tens of meters during shaking which later induced local beach sinking.

On the southern rim of the Buena Vista swamp, in the epicentral region, the pressure of the escaping water–sand mixture was high enough to unroot fully-grown coconut trees. Sand venting was also reported in ploughed papaya and sugarcane fields at Las Manoas estate, and particularly at Campo Alegre (on the northeast side of Cariaco) where 20–30 cm thick sand blows were spotted (deduced diameter of sand blows would be in the order of 2 to 3 m). There, almost all dirt-road embankments were damaged by lateral spreading, opening deep cracks that paralleled road alignment. Perception of evidence of liquefaction out of anthropologically modified zones was nearly impossible because large areas are constantly flooded and underwater, such as the Buena Vista and Campoma swamps that cover about half of the Cariaco sedimentary basin. However, it was common to observe slabs of riverbank that slid down to or laterally

Fig. 10. Response spectra (damping factor 5%) for three type-profiles of Cariaco: type-profiles 1 and 2 correspond to the representative structure of profiles A and B (Fig. 9), while the type-profile 3 is located at the northeastern end of profile A, where the thickness of the Quaternary sediments decreases (for details see Table 2). The thin and thick lines correspond to the response on the bottom and on the top of the sediments, respectively. The accelerogram used is a horizontal component (recorded on stiff sediment at 10.6 km distance to fault rupture) of the 1979 (Ms 6.9) Imperial Valley earthquake at an azimuth of 140°, which had a rupture mechanism similar to the 1997 Cariaco earthquake.

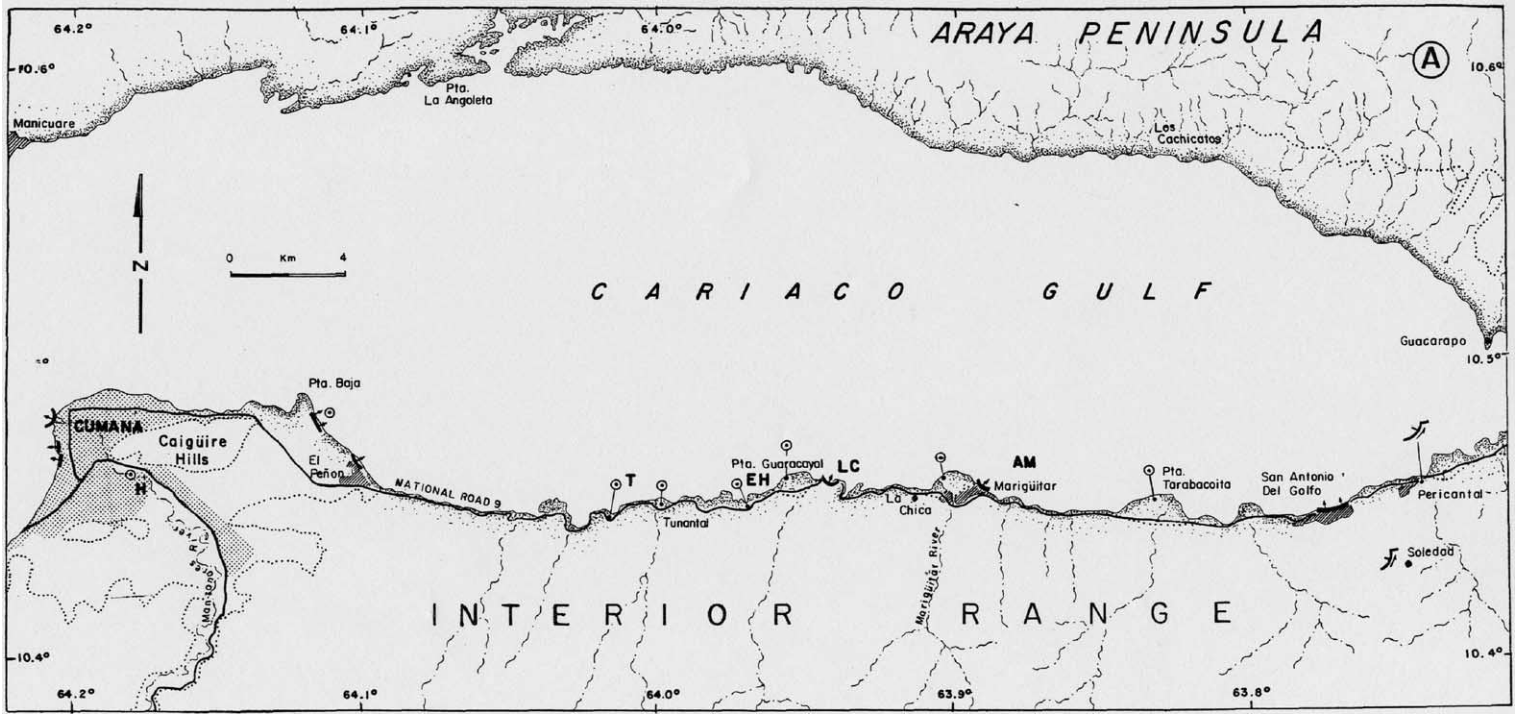

Fig. 11. Induced effects by the Cariaco earthquake around the Cariaco Gulf (A), and around its eastward continuation, the Cariaco sedimentary basin (B). T = Tocuchare, EH = Ensenada Honda, C = road 9 (north of Cariaco), LC = Calzadilla beach, ACA = Aquacam C.A., AM = Atún Margarita fish cannery, H = Veteran Hospital, Cumaná. Qal = Quaternary alluvial sediments, Ms = Mesozoic sedimentary rocks, Mm = Mesozoic metamorphic units.

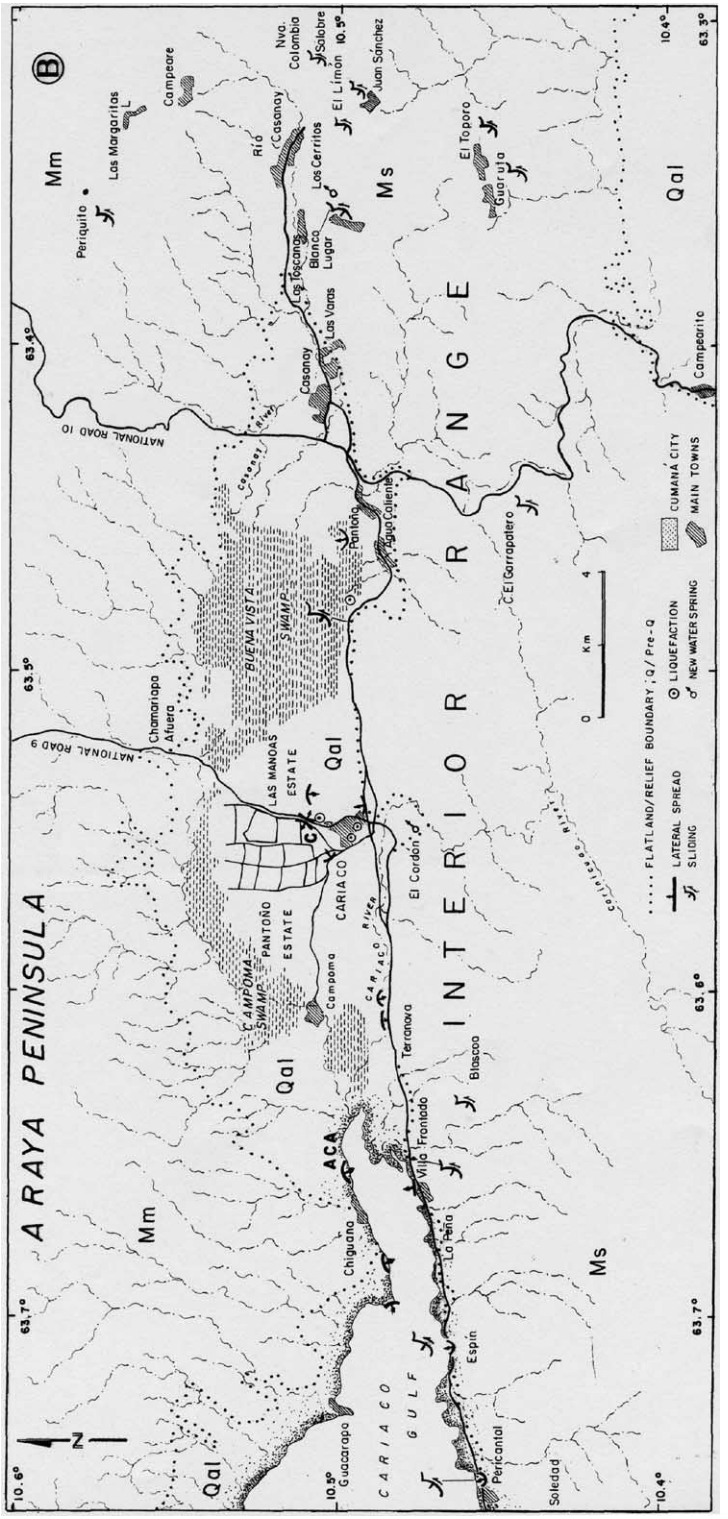

Fig. 11 (*continued*).

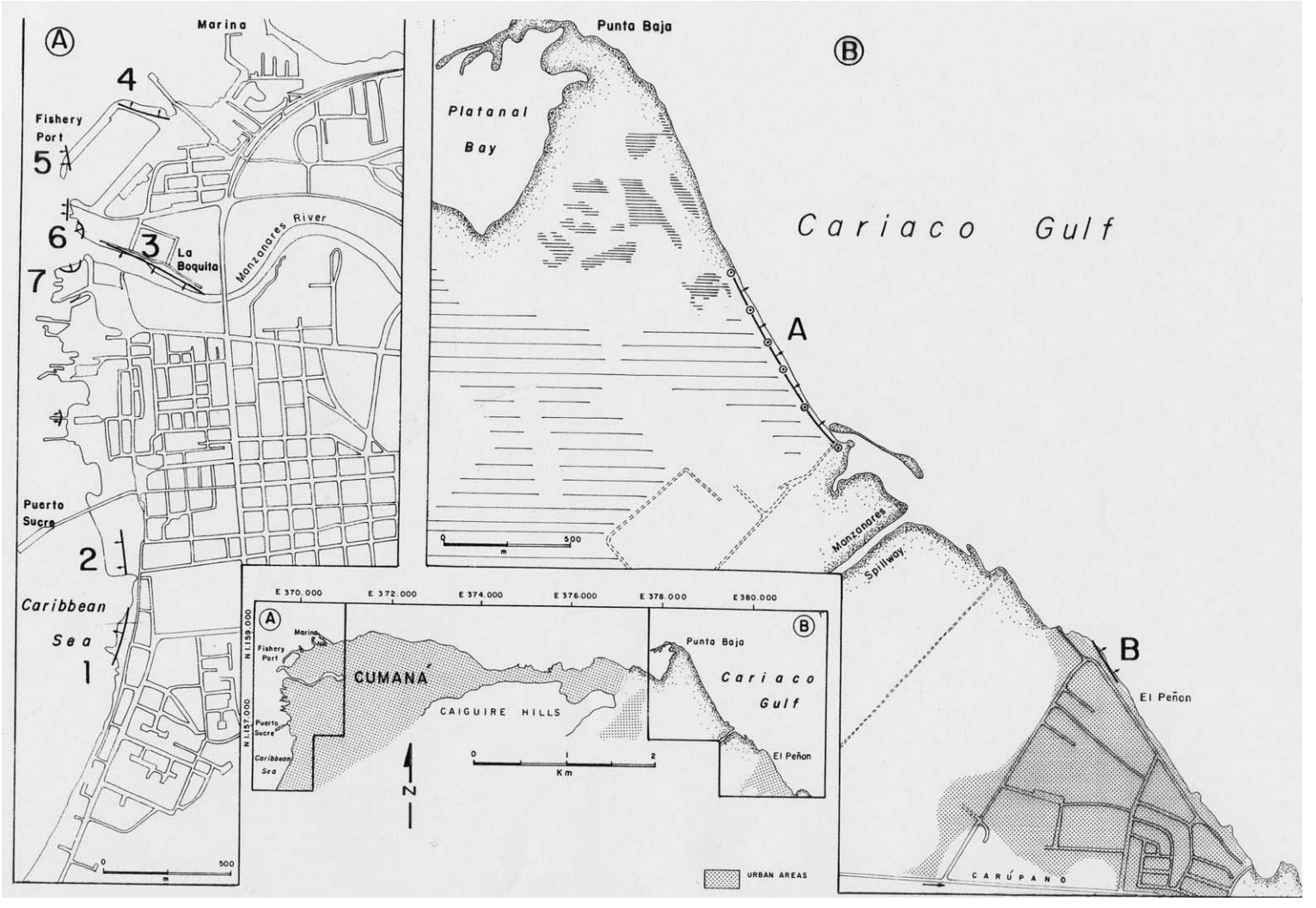

Fig. 12. Induced effects by the Cariaco earthquake along the shoreline in the city of Cumaná: (A) in the harbor district to the west and (B) the El Peñon area to the east; arrows indicate the direction of sliding. Numbers coincide with the description of the locations in the text.

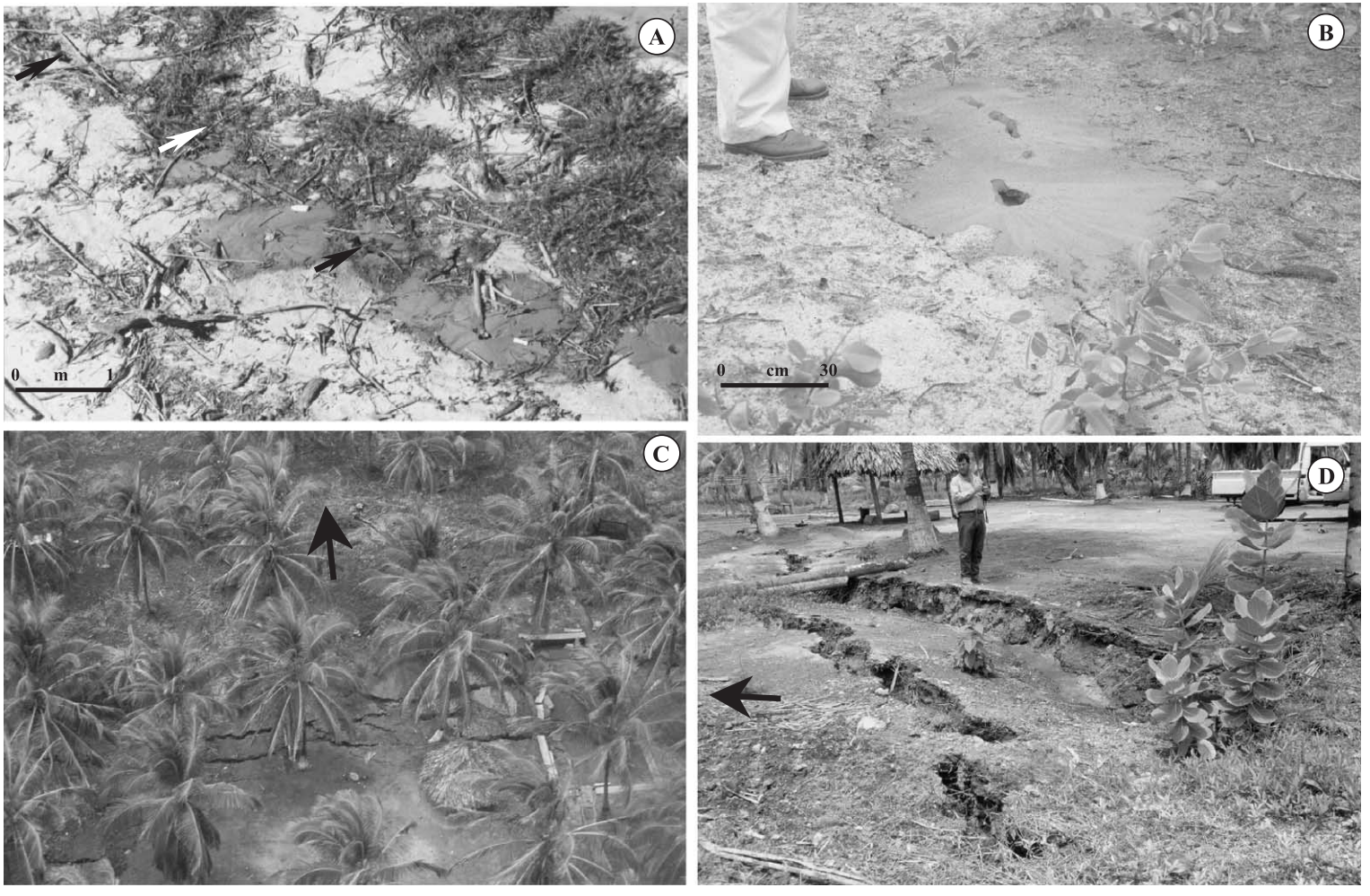

Plate 1. (A) Aligned sand blows vented through an open-fracture related to sea-front relaxation on the Punta Baja beach, east of Cumaná and NW of El Peñon (for location, refer to Fig. 11c); (B) detail of one of those aligned sand blows; (C) bird's-eye view of northward lateral spreading of almost flat-lying ground of a coconut plantation at the Piragua pool, on the southeastern edge of the Buena Vista swamp, next to the surface rupture of the Cariaco 1997 earthquake (arrow indicates the direction of sliding); and (D) detail view to the east of previous locality exhibiting clockwisely rotated slabs over a shallow liquefied layer. Also notice water shallowness in the southernmost crack.

moved into the creek bottom, regardless of bank height, such as along the Cariaco River between Cariaco and Terranova. Occasionally, where riverbanks were high, they toppled into the river. Most embankments of small and narrow earthen canals (generally less than 1 m high and typically less than a couple of meters wide) along discrete portions also cracked and moved laterally, either inwards or outwards. Lateral spreading also damaged national road 9 for a 500-m-long stretch just north of Cariaco (Fig. 11B). Here, earthen embankment failed because it moved laterally to both sides towards two nearby abandoned water-filled gravel pits dug during road construction.

Within the town of Cariaco, vent fractures and aligned sand blows were reported in the Brekerman, Bermúdez and Las Flores streets (for location, refer to Fig. 13). This southern sector of the town (paralleling a very shallow creek located south of the town) was strongly affected by lateral spreading, which had associated liquefaction. Surface gradient was almost flat (slightly inclined south), but houses within a stripe of two blocks in width and few hundred meters in length were severely damaged by water pressure that cracked them all and broke up floor concrete slabs. The affected houses were generally self-constructed one-story concrete frame masonry structures, built without any seismic-resistant design. Geotechnical studies in this area identified the occurrence of alluvial sand layers confined between clays of low plasticity.

On the Cariaco–Campoma road, the road embankment near a bend also failed by lateral spreading, producing the typical road edge failure (Fig. 11B). Getting away progressively to the west from the epicentral area, liquefaction features were spotted at Punta Cachipo (west of Chiguana) in association with sea-front relaxation on the northern coast of the Cariaco Gulf (Fig. 11B) and at several delta plains

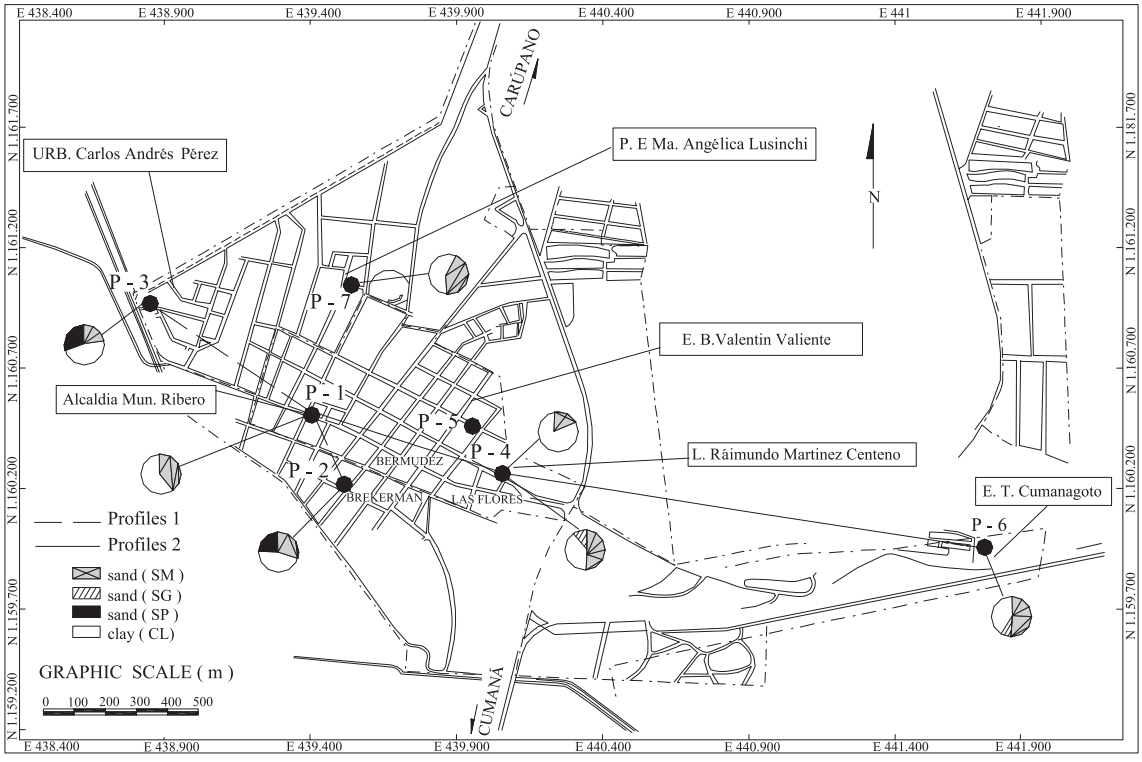

Fig. 13. Map of Cariaco with the location of geotechnical drillings and their respective soil type percentages (for details of sand layers see Table 3). Surface evidence for liquation has only been observed between Brekerman, Las Flores and Bermúdez streets in the south of the town. The location of the geotechnical profiles 1, running from drilling P2 in the south to drilling P3 in the northwest and profile 4, running from drilling P1 in the center to drilling P6 in the southeast (Fig. 14) is indicated.

on the southern seashore, such as Punta Tarabacoíta, Punta Monte Cristo (NW of Marigüitar), Punta Guaracayal, Tunantal and Punta Baja (Fig. 11A); this latter just being east of Cumaná. All these active Holocene alluvial plains exhibited sand blows. The largest sand blows were observed at the delta of the Marigüitar River (at Punta Monte Cristo, next to Maigualida beach), measuring 4–5 m across at about 50 km west of the reported epicenter (Plate 2A and B). On the Punta Baja sand barrier (corresponding to the present beach) sand blows reached 1 m in diameter (Plate 1A and B). But some few meters in land, within the floodplain of the Manzanares spillway canal, their size dropped below 30 cm. On the beach, an over 800-m-long crack system paralleling the seashore exhibited a very narrow (few centimeter wide) graben-like geometry (A in Fig. 12B). Frequently, those cracks had smelly gray sand venting associated; and occasionally exhibited aligned sand blows for over few meters in length (Plate 1A), as those described by Audemard and De Santis (1991). The graben-like cracks resulted from sea-front relaxation that seems to have eased formation of those 1-m-across sand blows in comparison to those reported few hundred meters away inland. At the auxiliary (artificially induced) delta mouth of the Manzanares River, 30-cm-across sand blows were spotted under brackish water less than 10 cm deep.

Southeast of the auxiliary spillway of the Manzanares river, the fisherman village of El Peñon, showed damage to houses sitting on the former beach (B in Fig. 12B). Parallel-to-the-shore cracking cuts across about 10 houses and hydraulic fills next to the shoreline, for a distance of the order of 150 m. All these are fisherman dwellings that are self-constructed, concrete-framed masonry houses but with no seismic-resistant considerations. Besides, fills were originally hand-made that are bounded by walls of poor or defective quality (mostly lacking good mortar).

The farthest most evidence of lateral spreading were found on the El Guapo coast, south of the seaport area (Puerto Sucre) on the western seashore of Cumaná (1 in Fig. 12A). Sea-front relaxation damaged houses (of similar construction type to those in Cariaco and El Peñon) over a distance of 180 m. The hydraulic fill of the southern part of the seaport facilities (with some warehouses above; Puerto Sucre, 2 in Fig. 12A) also moved slightly seaward, inducing surface cracking for almost 200 m in length. Further north on this western seashore of Cumaná, El Dique sector (La Boquita) underwent riverbank lateral spread for few hundred meters, damaging some 50 poorly constructed dwellings (3 in Fig. 12A). Individual crack opening could reach 0.50 m and might total over 1 m of lateral displacement across several subparallel cracks. North of that, the earth embankment of the fishery port was affected by lateral spreading at two sites: (a) along an east–west stretch near the port abutment (4 in Fig. 12A) and (b) at the tip of the port (5 in Fig. 12A and Plate 2C). Partial collapse of the pier appears not to be influenced by quality of construction. Conversely, it is very likely that collapse of the rock embankment at the port tip may be related to a huge submarine slump that affected the mouth bottom of the actual Manzanares River. This huge slide might be responsible for damage to a dry dock on the right riverbank (6 in Fig. 12A and Plate 2D) and to the ferryboat jetty on the opposite bank of the Manzanares river mouth (7 in Fig. 12A). Likeliness of this mass-wasting process is very high since the Manzanares River pours its water into the very east end of the deep-marine Cariaco trough that lies just west of the river mouth. Along the Manzanares River inland, small sand blows were seen near the Veteran Hospital (the former Anti-tuberculosis Hospital of Cumaná), located both south of the river and southwest of the Caigüire hills (H in Fig. 11A).

Though lateral spreading affected natural features at many places (very particularly riverbanks and sandy beaches but very rarely marine cliffs like east of Chiguana (Plate 3A) in the northern coast of the Cariaco Gulf), it also damaged cultural features very frequently. Hydraulic fills along both Cariaco Gulf coasts were heavily damaged, extending as far west as Los Capotes (Calzadilla beach, LC in Fig. 11A; Plate 3B). Here, a sea viewpoint was affected by free-face relaxation of the artificial fill. But the largest damages with great negative economic impact by lateral spreading were suffered by the seaside promenade of San Antonio del Golfo and the fish cannery at Marigüitar (Atún Margarita) on the southern coast, whereas only the shrimp farms of Aquacam, C.A. located east of Chiguana on the north coast (Fig. 11B) were deeply damaged by lateral spreading (with surface sand venting) of the southern earthen embank-

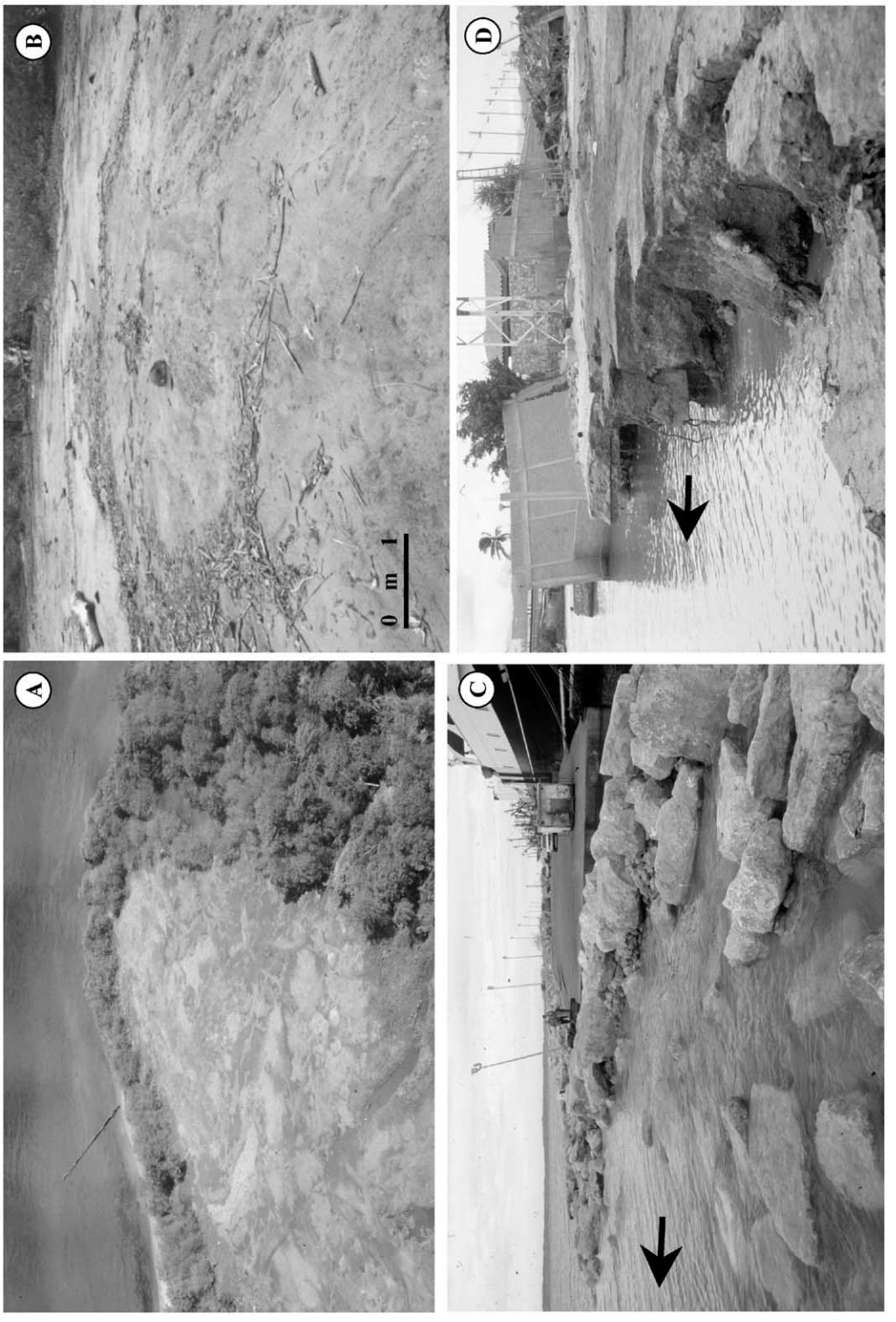

Plate 2. (A) Bird's-eye view of sand blowing at the Marigüitar delta, next to the Maigualida beach on the southern coast of the Cariaco Gulf (for location, refer to Fig. 11); (B) detail of one of those isolated sand blows measuring between 4 to 5 m across; (C) collapse of rock embankment at the tip of the fishery port located on the western coast of Cumaná and near the Manzanares river mouth; and (D) sliding of hydraulic fill edge and rails at a dry dock induced by submarine slumping at the Manzanares river mouth (for location refer to Fig. 12).

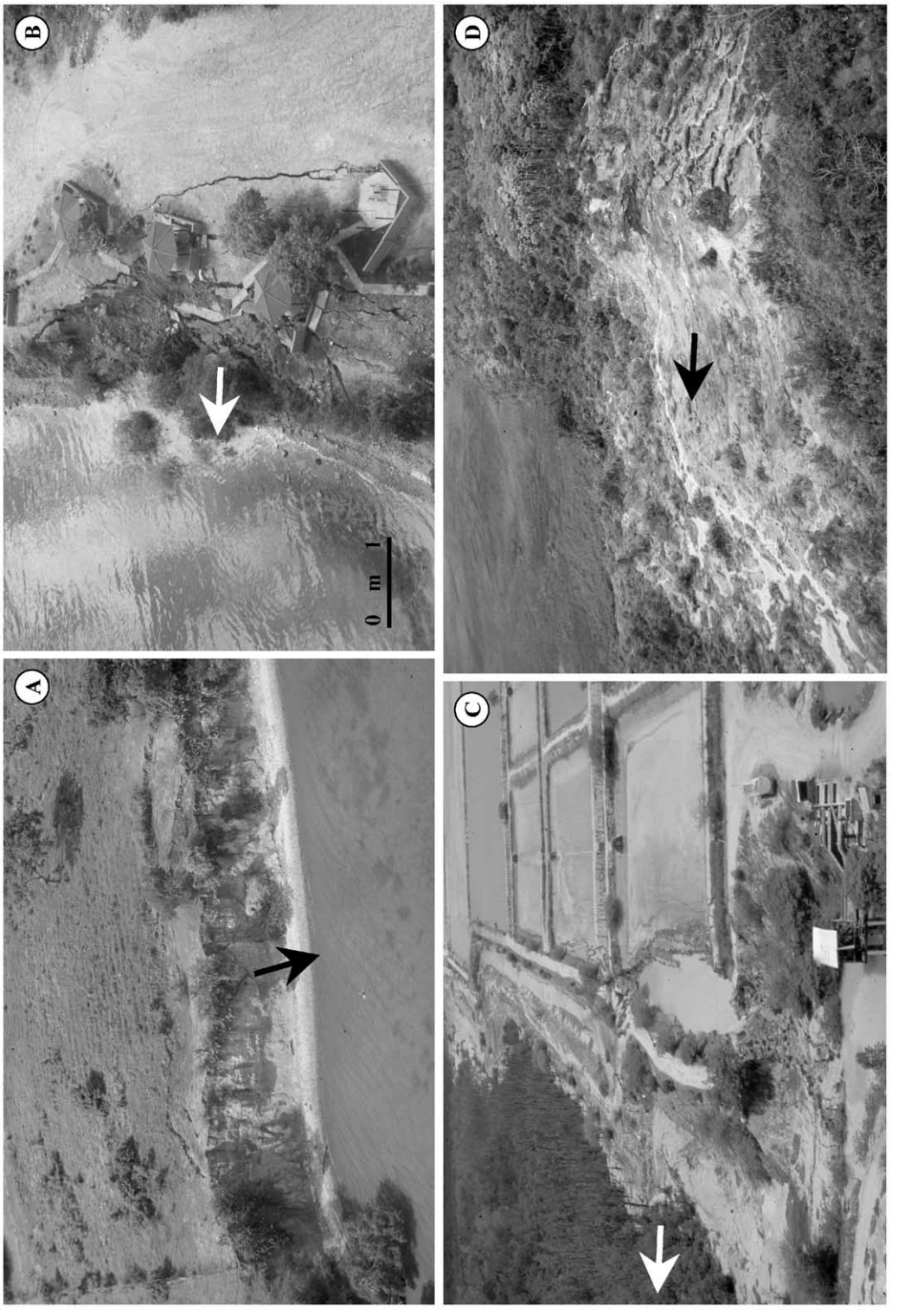

Plate 3. (A) Small lateral spreading in few-meter-high Plio-Pleistocene cliffs on the northern coast of the Cariaco Gulf, nearby Chiguana (for location, refer to Fig. 11); (B) lateral spread affecting small resting area sitting on artificial fill, at the Calzadilla beach, on the southern coast of the Cariaco Gulf; (C) bird's-eye view of seaward lateral spreading of the southernmost earth embankment of the Aquacam C.A. shrimp farm, east of Chiguana; and (D) sliding of travertine pools originally capping the El Pilar fault scarp developed on Mesozoic mudstones at the Aguas Calientes farm. To the south, some unbroken pools can be spotted, whereas travertine blocks are piling up to the north (left). Arrows indicate the direction of sliding.

ments due to a free-face effect on the south (Plate 3C). However, other sites displayed fracturing parallel to seashore at lesser extent, such as Villa Frontado and several localities on the western coast of Cumaná already mentioned.

From these observations, it can be stated that: (a) liquefaction and lateral spreading induced by the Cariaco 1997 earthquake occurred where all controlling factors concurred: in the active Holocene alluvial/deltaic plains and seashore sand barriers; and (b) liquefaction distribution during the Cariaco earthquake coincides with areas of larger intensities (MMI VI to VIII; compare Figs. 2 and 11). Additionally, it also reveals two relevant aspects: (1) since liquefaction distribution is pulled to the west with respect to the epicenter, the monodirectionality to the west (or highly asymmetric bidirectionality) of the rupture propagation proposed by Audemard (1999, under review, a) and verified by numerical modeling (Mendoza, 2000), and consequently of the energy as well, appears to be supported from this unequal distribution, though liquefaction-prone areas are also more abundant to the west of the epicenter, around the Cariaco Gulf; (2) although size and frequency of occurrence of liquefaction/lateral spread features diminishes away from the epicenter, as expected, a great amount of lateral spreads has affected the either natural or anthropologically modified seashore areas of Cumaná and suburbs in comparison with the surroundings, which reveals that the Cumaná subsoil presents particular soil conditions.

4.2. Geotechnical characterization of the liquefied soils in Cariaco

We will focus on the geotechnical conditions of the southern part of Cariaco, particularly in the Bermúdez, Flores and Brekerman streets (Fig. 13) along two profiles, one in the west and another from the center towards the southeastern edge of the basin (Fig. 14). In total, seven boreholes were studied regarding lithology, compactness (NSPT), thickness and fine content of the sand layers. The most important geotechnical characteristics of the subsoil sand layers are indicated in Table 3. Although superficial evidence for liquefaction was observed only in the southern part of Cariaco between the Bermúdez, Las Flores and Brekerman streets (De Santis and Hernández, 1999), a qualitative estimation of the liquefaction potential following Seed's methodology (Seed and Idriss, 1971), considering an acceleration of 0.3 g, was done for all boreholes.

As no accelerogram from the epicentral region was available, the liquefaction potential was estimated for every single sand layer identified in the geotechnical boreholes, using three different levels of seismic acceleration: 0.10, 0.15 and 0.3 g, following Seed's methodology (Seed and Idriss, 1971). The results indicate a liquefaction potential for all drillings at different depth levels, except the P6 drilling, which is located close to the basin edge (Figs. 13 and 14). They also show that a higher number of sand layers than observed should have liquefied if the acceleration would have been above 0.3 g. The critical parameters for the occurrence of liquefaction are a fine content between 5% and 30%, 100% saturation with water, and NSPT values below about 25 blows. Furthermore, the calculations indicate that no layer would have liquefied if the acceleration would have been lower than 0.1 g. Therefore, we suppose that the seismic acceleration in Cariaco could have ranged between 0.15 and 0.3 g. The recorded maximum horizontal acceleration in Cumaná, some 80 km west of the epicenter, was 0.17 g on consolidated Plio-Pleistocene sediments (FUNVISIS, 1997).

In Cariaco, liquefaction was observed in sand layers belonging to sediments deposited in abandoned meanders. These sediments represent probably the youngest materials identified in the subsoil of Cariaco, in areas near to Cumaná and around the Cariaco Gulf. Seed's methodology for estimating liquefaction potential should be used as a first approximation for microzoning purposes, since it is a predictive method of easy application relying on blow counts from the SPT test, the fine content of sands and the maximum acceleration expected in the region. Nevertheless, the limitations of this method must be considered when interpreting the results. Therefore, more refined analyses are necessary for more reliable results for seismic microzoning assessments.

In average, about 40% of all dwellings in Cariaco were heavily damaged or collapsed during the earthquake. In the central region of Cariaco, over 60% of them were damaged, whereas towards the southeast, close to the surface rupture and on the more consolidated sediments, only 20% of the dwellings were

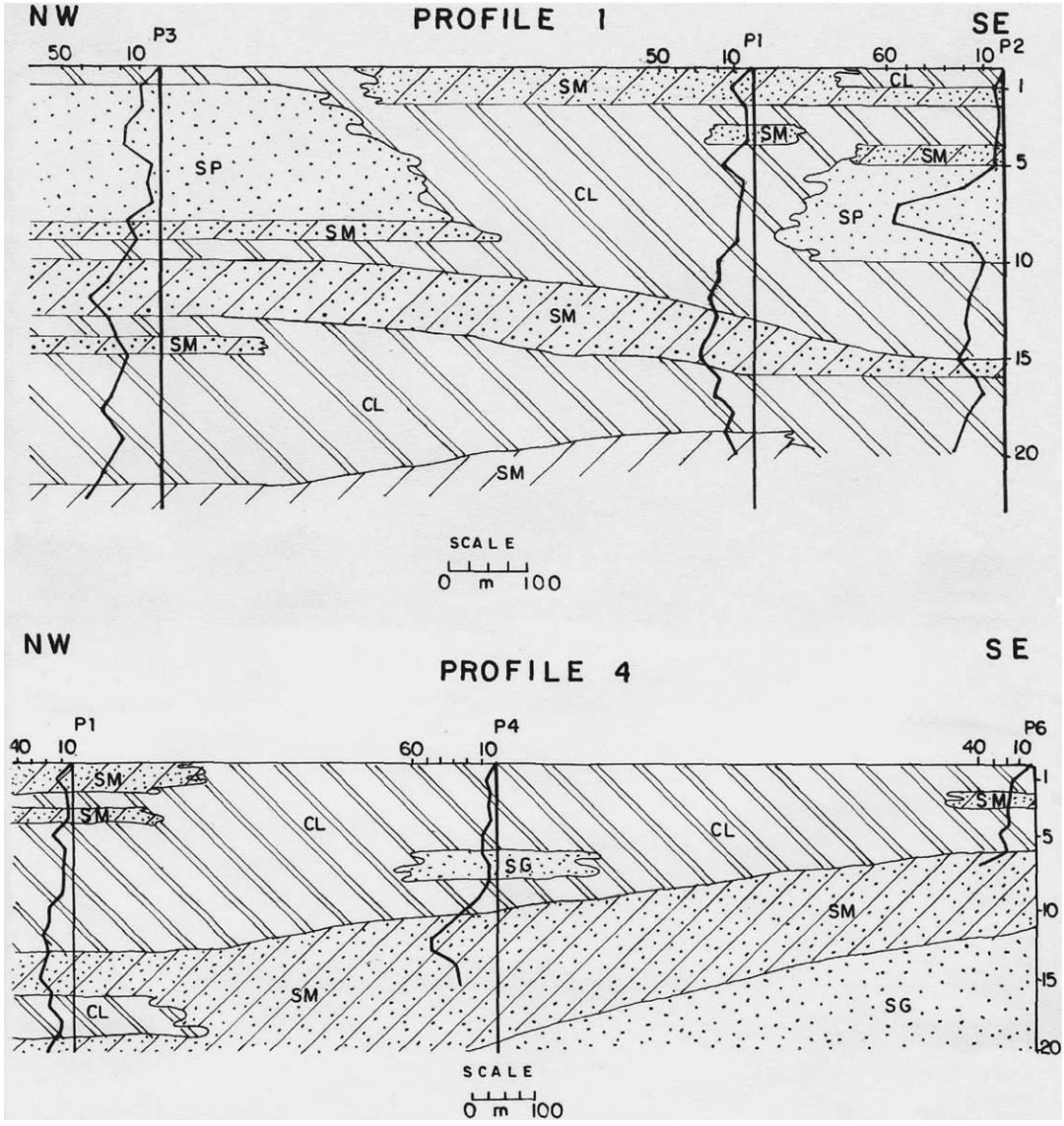

Fig. 14. Profiles summarizing the geotechnical information in Cariaco crossing drillings P3, P1 and P2 from NW to SE (profile 1, top) and P1, P4 and P6 from NW to SE (profile 4, bottom). The number of SPT counts are indicated for each drilling; CL = clay, SM = silty sand, SP = poorly sorted sand, SG = sand with gravel.

damaged (Gámez et al., 1999). Nevertheless, we cannot establish a direct correlation between the predominant periods (Fig. 5), S-wave velocities (Fig. 9) and liquefaction potential (Fig. 13) and the damages in Cariaco, as many of the collapsed structures were poorly maintained "bahareque" houses, and the damage distribution is strongly influenced by the type and quality of construction.

4.3. Sliding

The hilly areas near the epicenter were extensively affected by sliding but of rather small size. Excluding the probable submarine slump that affected the mouth of the Manzanares River at Cumaná, slides are modest in size and are rarely over a 100 m across. Displacement is in the order of few centimeters, except for: (a)

Table 3
Borehole profiles in Cariaco indicating the most important geotechnical parameters of the sand layers with respect to their liquefaction potential (for location see Fig. 13)

Sand layer (depth)	Thickness (m)	Classification SUCS	N-SPT (average)	% Fine	Liquefaction potential (Seed)	Saturation (%)	Confined by clays
Los Bloques (INAVI urbanization)—P3							
1.55–8.55	7	SP	12	8.14	Yes	100	No
12.5–13.5	1	SM	29	12.78	No	100	No
14.5–16.5	2	SM	22	28.00	No	100	Yes
Medicatura (Preescolar María Angélica Lusinchi)—P7							
0.55–2.55	2	SM	4	40.50	No	Partial	No
3.55–4.55	1	SM	8	31.50	Yes	100	No
6.55–8.55	2	SM	10	18.34	Yes	100	Yes
10.5–11.5	1	SM	18	27.00	Yes	100	Yes
14.5–18.5	4	SM	24	18.44	Yes	100	Yes
19.5–20.5	1	SM	29	31.00	Yes	100	No
Valentín Valiente School—P5							
0.55–1.55	1	SP	7	8.13	No	Partial	No
2.55–3.55	1	SM	9	30.49	Yes	100	No
5.55–6.55	1	SP	20	11.10	Yes	100	Yes
9.5–10.5	1	SM	9	19.17	Yes	100	Yes
Raimundo Martínez Centeno School—P4							
6.55–7.55	1	SG	6	5.86	Yes	100	Yes
9.55–13.5	4	SM	38	21.38	No	100	No
13.5–15.5	2	SG	28	11.57	Yes	100	No
Cariaco Major Office—P1							
0.55–2.55	2	SM	8	39.55	No	Partial	No
3.55–4.55	1	SM	5	38.30	No	100	Yes
12.5–15.5	3	SM	25	22.67	Yes	100	Yes
19.5–20.5	1	SG	13	36.90	No	100	No
Brekerman Street—P2							
1.55–2.55	1	SM	3	29.20	Yes	100	Yes
4.55–5.55	1	SM	20	11.10	Yes	100	No
5.55–8.55	3	SP	44	3.55	No	100	No
8.55–10.5	2	SP	14	4.75	Yes	100	No
Cumanagoto School—P6							
2.55–3.55	1	SM	19	22.00	No	Partial	Yes
5.55–6.55	1	SM	19	21.00	No	Partial	No
6.55–10.5	4	SM	95	27.25	No	Partial	No
13.5–15.5	2	SG	100	11.86	No	100	No

Surficial evidence for liquefaction was observed only at drilling P2 in the Brekerman Street. The level of seismic acceleration considered for the estimation of the liquefaction potential is 0.3 g. NSPT is normalized to 60% of blow counts from SPT tests.

the slides affecting roads where cuts fell down on the road and uncompacted fill of road bench slid downslope; and b) the earthquake-triggered slide that destroyed travertine staircased pools at the Agua Caliente farm where travertine blocks slid down along slope of the El Pilar fault scarp (Plate 3D) and highly calcareous milky-like waters were poured into the Buena Vista swamp for several days.

Many roads were damaged by slides (landslides, rockslides and rockfalls) in different degrees at several places (for more details, refer to FUNVISIS, 1997 and MTC, 1997): El Limón (east of Río Casanay), El

Salobre (south of Nva. Colombia), El Toporo (7 km south of Río Casanay), Espín (between San Antonio del Golfo and Villa Frontado), La Ceiba, Pantoño-La Pica (east-facing slope of the Garrapatero hill), Pericantal (between San Antonio del Golfo and Villa Frontado), Pericantal-Paradero local road, Río Abajo (Villa Frontado-Blascoa road). Many of these roads run on top or along steep slopes of hills and ranges. Also self-constructed "bahareque" or concrete-framed dwellings, churches and schools were affected by mass instabilities on hilly areas. Blanco Lugar and Juan Sánchez are among those being damaged most. Sliding was also reported on uninhabited hillslopes, such as at: El Paraiso hill at Guaruta (7 km south of Río Casanay) and near Periquito (6 km north of Río Casanay).

4.4. Other effects

Two very common associated effects have been mentioned and precisely described by locals but not witnessed by authors of this paper except for very few cases that suggest that reported facts are likely to have occurred, namely sea-front retreat and water table changes.

4.4.1. Sea retreat

Almost all along the coasts of the Cariaco Gulf, inhabitants of fisherman or seaside settlements reported that during the shaking the sea receded few tens (30 to 50) of meters and then came back rather smoothly to its original position, and eventually went farther beyond inland. In Cumaná, where seawaters are shallow for over hundreds of meters, people reported that water retreated about 100 m. This allowed estimating that waves were in the order of 1 m high.

This initial seawater retreat may be explained if slip along the El Pilar fault during the Cariaco 1997 earthquake in combination with the relative position of the water body of the Cariaco Gulf with respect to the fault is taken into account. The water body is located mainly north of the fault and the fault moved dextrally (Fig. 1), thus pulling the gulf seafloor towards the east and generating a water deficiency on the opposite side (to the west). The sea retreat was noticed very clearly west of San Antonio del Golfo. Sea retreats have been evidenced during several historical earthquakes in the region (see Audemard, under review, b). Sea retreat during the Cariaco 1997 earthquake could not be imputed to the submarine slump west of Cumaná because the effects should have been more local and not so widespread in the Cariaco Gulf.

4.4.2. Water table changes

Many changes in water table elevation have been reported. Some reports are reliable like the following one: Audemard (1999) personally witnessed the lack of running water at the Piragua pool (north of the town of Agua Caliente) in the afternoon of Tuesday July 15, 1997, which had returned next morning (1 week after the main shock). Also, a natural spring broke up at El Cordón de Cariaco, south of Cariaco and at the foot of the limestone-rich hills lying to the southwest (Fig. 11B). After elderly locals' accounts, this spring dried up during the Cumaná 1929 earthquake. To drain water from the flooded town and out of their septic tanks, a backhoe-dug ditch was excavated along the main street in July 1997. In April 1998, fresh water was still running across the town, in the open ditch.

Furthermore, water flow dropped or dried out at warm springs of Cachamaure-San Antonio del Golfo, at San Antonio del Golfo and at two warm springs at El Volcancito (both before the earthquake). On the contrary, flow increased at Blanco Lugar where a vertical water jet started 3 h before main shock. In addition, that cold-water spring became warm, as stated by local observers from Periquito.

5. Summary and conclusions

Permanent ground deformations were observed, not only along the surface rupture (see Audemard, under review, a), but also at sites affected by induced effects like soil liquefaction, lateral spread, and slides. Liquefaction and lateral spreading induced by the Cariaco 1997 earthquake occurred where all controlling factors concurred, restraining them essentially to the active Holocene alluvial/deltaic plains and coastal sand barriers. The area of distribution of these phenomena coincides with areas of larger intensities (MMI VI to VIII). The induced effect distribution shows a similar pattern to the isoseisms in the epicentral area: a strong W–E elongation along the

Cariaco Gulf and its eastward extension into the Cariaco sedimentary basin (Figs. 2 and 11). This directivity in the attenuation may be explained by the regional, WSW–ENE to E–W oriented, structural trend (folds, major faults, bedding and foliation) as well as by the orientation of major geomorphic units such as mountain chains (Araya and Paria peninsulas and Interior Range) and sedimentary basins (Cariaco Gulf and basin). Additionally, the induced effects seem to extend farther to the west than to the east (with respect to the epicenter), which might be explained by an asymmetrically west-directed rupture propagation as proposed by Audemard (1999, under review, a) and modeled by Mendoza (2000). Sliding was mostly confined to the hilly area south of the epicenter and frequently damaged the local road system. The slides rarely exceeded a size of 100 m across, with the exception of a probable submarine slump at the river mouth of Manzanares River in Cumaná. Other effects, like sea retreat or water table changes, were frequent but did not generate serious damage.

The soil conditions in Cariaco, the town most affected by the 1997 Cariaco earthquake, were investigated in detail by different methods. The results of microtremor measurements indicate predominant soil periods between 0.6 and 1.2 s for Cariaco, without clear recognizable patterns in the center, but decreasing values towards the northeast and along the fault rupture (Fig. 5). Two bedrock sites to the south showed distinctly lower predominant periods in the range of 0.3 s. In Cumaná, predominant periods exceed 1 s at coastal lowlands and close to the Manzanares River (Abeki et al., 1998). The location of the long period sites correlates well with the damage distribution from the Cariaco earthquake, some 80 km from the epicenter (Lang et al., 1999).

This paper presents results from a shallow seismic refraction survey that was performed in Cariaco in order to generate detailed input information for the modeling of the dynamic behavior of the soil. The soil sequence, which correlates to the Quaternary sediments, exhibits S-wave velocities below 700 m/s, exceeding 90 m in depth in great parts of the town (Fig. 9). The boundary with the underlying Tertiary sediments (or the weathered top of Cretaceous limestones), with S-wave velocities of about 700 m/s (P-wave velocity of 2.500 m/s), could not be defined for the whole town, as it could be observed only on some seismic lines at depths between 60 and 90 m, essentially in the southern part of the town. We therefore assumed the depth of the "hard soil" (or rock equivalent) at 60 and 90 m for three type profiles, for which seismic response spectra of the acceleration were calculated (Fig. 10). As a principal result, energy is absorbed to about 0.4 s and amplification occurs between 0.4 and 3 s, with acceleration values exceeding 0.5 g. The frequency ranges with observed amplification do not coincide well with the measured predominant periods. We do not consider the amplification effects as the main cause for the damage occurred in Cariaco during the 1997 event, as the one to two story dwellings have a much shorter predominant period. The high percentage of damage in Cariaco (about 40% of all dwellings were heavily damaged or collapsed during the 1997 Cariaco earthquake; Gámez et al., 1999) is due to inappropriate construction quality of self-constructed concrete-framed masonry structures and/or poor maintenance of century-old "bahareque" houses.

In general, the observed damage was due to an inadequate behavior of the constructions because of inappropriate design of the structural elements and beam-column joints, as well as the high level of acceleration, that introduced large displacements according to the dynamic models. A strong correlation between the soil characteristics and the damage occurrence was reported for southern Cariaco. Here, soil liquefaction occurred on recent sediment accumulation from the Cariaco River, which flows along the southern edge of the town. The geotechnical profiles indicate sand layers being located within low plasticity clays. Considering the thickness of the soft soils reported for Cariaco in the order of 90 m, the 0.3 g value estimated for the maximum ground motion using Seed's method might be a lower bound to the possible values, even more, if we keep in mind that the records obtained in Cumaná, some 80 km from the epicenter and located on consolidated sediments, already reported 0.17 g (FUNVISIS, 1997). The new seismic building code (COVENIN, 2001) will hopefully induce seismic microzoning assessments in Venezuela, as local soil conditions will be more important to the requirements made in this code.

Acknowledgements

Seismic refraction measurements were made possible by using the Geometrics seismic recorder of Freie Universität Berlin (FUB)—special thanks to P. Wigger and S. Lüth. These studies were mainly funded by emergency plan supported by PDVSA. We thank A. Singer for encouraging most of the studies reported here. FUNVISIS staff M. Bonato, L. Acosta, L. Vasallo, C. Grimán, A. Hernández and N. Reyes participated in the macroseismic evaluation. H. Duque, G. Malavé, J. Alvarellos (INTEVEP), A. Pernía and N. Reyes (FUNVISIS) contributed to the seismic measurements and V. Rocabado (FUNVISIS) to microtremor measurements and processing. We thank M. Peña for her excellent china-ink drafting. CAVIM did explosive handling for seismic energy. Accelerograms used for dynamic modeling are from PEER Strong Motion Database. Reviews of S. Richwalski, P.-Y. Bard and one anonymous reviewer contributed substantially to the improvement of the manuscript.

Appendix A

Locations evaluated for the macroseismic map shown in Fig. 2, labeled as in the map, indicating the assigned intensity and the geographic coordinates.

Location	#	MMI	LAT	LONG
Agua Caliente	87	8	10.5	– 63.49
Agua Fría Abajo	78	7	10.47	– 63.26
Agua Fría Arriba	26	5	10.46	– 63.26
Aragua de Maturín	15	5	9.97	– 63.48
Araya	31	5	10.57	– 64.25
Arenas	7	4	10.25	– 63.89
Barcelona	30	5	10.13	– 64.68
Blanco Lugar	89	8	10.49	– 63.36
Boca de Río	58	6	10.46	– 64.17
Caicara	3	4	9.82	– 63.6
Campearito	59	6	10.37	– 63.4
Campoma	90	8	10.51	– 63.61
Cangrejal	85	8	10.47	– 63.32
Cariaco	99	8	10.5	– 63.55
Caripe	27	5	10.18	– 63.48
Caripito	28	5	10.12	– 63.08
Carrizal de la Cruz	72	7	10.49	– 63.51
Carúpano	60	6	10.67	– 63.23
Casanay	100	8	10.5	– 63.43

Appendix A (*continued*)

Location	#	MMI	LAT	LONG
Catuaro	33	5	10.4	– 63.49
Cerro Campeare	75	7	10.5	– 63.32
Cumacatal	35	5	10.48	– 63.22
Cumaná	61	6	10.45	– 64.17
Cumanacoa	1	4	10.26	– 63.92
Chacopata	54	5	10.7	– 63.83
Chamariapa Afuera	55	6	10.54	– 63.53
Chiguana	96	8	10.49	– 63.68
El Cautal	92	8	10.51	– 63.3
El Cautaro	91	8	10.49	– 63.27
El Limón	77	7	10.5	– 63.33
El Peñon	24	5	10.42	– 64.23
El Pilar	56	6	10.55	– 63.17
El Salobre	93	8	10.51	– 63.31
El Toporo	81	7	10.46	– 63.34
El Vicio	25	5	10.58	– 63.57
Ensenada Honda	22	5	10.45	– 63.97
Fundo La Coquera	70	7	10.48	– 63.65
Garrapatero	57	6	10.45	– 63.45
Golindano	66	6	10.45	– 63.89
Guaca	63	6	10.67	– 63.4
Guacarapo	65	6	10.5	– 63.73
Guamache	18	5	10.65	– 63.82
Guanaguana	21	5	10.07	– 63.6
Guaruta	73	7	10.45	– 63.34
Guiria	20	5	10.58	– 62.28
Irapa	10	5	10.58	– 62.58
Juan Antonio	64	6	10.35	– 63.35
Juan Griego	4	4	11.1	– 63.95
Juan Sanchez	82	7	10.49	– 63.32
La Asunción	5	4	11.05	– 63.87
La Ceiba	71	7	10.51	– 63.27
La Chica	41	6	10.45	– 63.92
La Funcia	42	6	10.45	– 63.47
La Pica	50	6	10.45	– 63.45
Los Altos	19	5	10.23	– 64.47
Los Capotes	52	6	10.45	– 63.94
Mariguitar	53	6	10.45	– 63.9
Maturín	6	4	9.75	– 63.17
Mochima	49	6	10.35	– 64.33
Nueva Colombia	84	8	10.52	– 63.31
Pampatar	23	5	11	– 63.78
Pantoño	94	7	10.48	– 63.45
Pinto de Punceres	11	5	9.92	– 63.3
Porlamar	12	5	10.95	– 63.85
Puerto La Cruz	8	5	10.22	– 64.62
Quiriquire	9	5	9.97	– 63.23
Río Abajo	13	5	10.43	– 63.61
Río Caribe	16	5	10.7	– 63.1
Río Casanay	69	7	10.52	– 63.33
San Antonio del Golfo	67	7	10.44	– 63.8
San Félix	34	5	9.95	– 63.65
San José de Areocuar	76	6	10.62	– 63.33

(continued on next page)

Appendix A (*continued*)

Location	#	MMI	LAT	LONG
San Juan Bautista	37	5	10.97	− 63.9
San Juan de Azagua	36	5	10.02	− 63.15
San Juan de Las Galdonas	29	5	10.72	− 62.83
Santa Ana	97	6	10.32	− 63.65
Santa Cruz	32	6	10.41	− 63.91
Santa Lucía	47	6	10.42	− 63.38
San Vicente	39	6	10.23	− 63.2
Saucedo	46	6	10.62	− 63.52
Soledad	51	6	10.59	− 63.54
Tacarigua	2	4	11.07	− 63.92
Terranova	83	7	10.48	− 63.62
Tucuchare	45	6	10.44	− 64.01
Tunantal	80	7	10.45	− 64
Tunapuy	43	6	10.57	− 63.1
Valle Solo	44	6	10.45	− 63.93
Villa Frontado	79	7	10.47	− 63.67
Yaguaraparo	40	6	10.57	− 62.83

References

Abeki, N., Watanabe, D., Hernández, A., Pernía, A., Schmitz, M., 1998. Microtremor observations in Cumaná City, Venezuela. In: Irikura, Kudo, Okada, Sasatani (Eds.), The Effects of Surface Geology on Seismic Motion. Balkema, Rotterdam, pp. 613–618.

Audemard, F.A., 1999. El sismo de Cariaco del 09 de julio de 1997, Edo. Sucre, Venezuela: nucleación y progresión de la ruptura a partir de observaciones geológicas. VI Congreso Venezolano de Sismología e Ingeniería Sísmica, Mérida, Venezuela (CD-Rom format), 15 pp.

Audemard, F.A., under review, a. Surface rupture of the Cariaco July 09, 1997 earthquake on the El Pilar fault, northeastern Venezuela.

Audemard, F.A., under review, b. Revised seismic history of the El Pilar fault, northeastern Venezuela, from the Cariaco 1997 earthquake and recent preliminary paleoseismic results.

Audemard, F.A., De Santis, F., 1991. Survey of liquefaction structures induced by recent moderate earthquakes. Bulletin of the International Association of Engineering Geology 4, 5–16.

Audemard, F.A., Machette, M., Cox, J., Hart, R., Haller, K., 2000. Map and database of Quaternary faults in Venezuela and its offshore regions. U.S. Geological Survey Open-File-Report 00-18. 79 pp. + map.

Bard, P.Y., 1999. Microtremor measurements: a tool for site effect estimation? In: Irikura, K., Kudo, K., Okada, H., Sasatani, T. (Eds.), The Effects of Surface Geology on Seismic Motion—Recent Progress and New Horizon on ESG Study, vol. 3. Balkema, Rotterdam, pp. 1251–1279.

Bellizzia, A. (coord.), Pimentel, N., Bajo, R., 1976. Mapa Geológico Estructural de Venezuela, escala 1:500.000. Ediciones FONINVES, Caracas.

Beltrán, C., Rodríguez, J.A., 1995. Ambientes de sedimentación fluvio-deltáica y su influencia en la magnificación de daños por sismos en la ciudad de Cumaná: II. Coloquio Internacional de Microzonificación Sísmica, Cumaná, Venezuela, FUNVISIS, unpublished, 12 pp.

Bonato, M., Hernández, A., 1999. Evaluación macrosísmica del terremoto de Cariaco de 1997 y ley de atenuación de intensidades. VI Congreso Venezolano de Sismología e Ingeniería Sísmica, Mérida, Venezuela (CD-Rom format), 6 pp.

Bonilla, R., López, O.A., Castilla, E., Torres, R., Marinilli, A., Annicchiarico, W., Garcés, F., Maldonado, Z., 2000. El terremoto de Cariaco del 9 de Julio de 1997. Boletín Técnico IMME 38, 1–50.

COVENIN, 2001. COVENIN 1756-98, Revisión 2001, "Edificaciones Sismorresistentes", Ministerio de Desarrollo Urbano, FUNVISIS.

De Santis, F., Hernández, R., 1999. Caracterización de los suelos que licuaron durante el sismo del 9 de Julio de 1997 en Cariaco, Estado Sucre. VI Congreso Venezolano de Sismología e Ingeniería Sísmica, Mérida, Venezuela (CD-Rom format), 10 pp.

FUNVISIS, 1994. Estudio Neotectónico y de Geología de Fallas Activas de la Región Nororiental de Venezuela. Proyecto Intevep 92-175. FUNVISIS' unpublished report for Intevep, S.A., 3 vol.

FUNVISIS, 1997. Evaluación preliminar del sismo de Cariaco del 09 de Julio de 1997, Estado Sucre, Venezuela (versión revisada). FUNVISIS, 123 pp. + 5 appendices.

FUNVISIS, IMME, UDO, Venezuelan Academy of Sciences, CAV, CIV-Sucre, 1997. The July 9, 1997, Cariaco, Eastern Venezuela earthquake. EERI Special Earthquake Report. EERI Newsletter 31, 1–8.

Gámez, M., Hernández, R., De Santis, F., 1999. Elaboración de un mapa de índice de daños durante el sismo ocurrido en Cariaco, Edo. Sucre, el 9 de Julio de 1997. VI Congreso Venezolano de Sismología e Ingeniería Sísmica, Mérida, Venezuela (CD-Rom format), 9 pp.

Grases, J., 1990. Terremotos Destructores del Caribe, 1502–1990, 1st ed. Orcyt-Unesco, Montevideo, Uruguay. 132 pp.

Kantak, P., Schmitz, M., Ramos, C., Montilla, A., Rojas, J., 1999. Bericht ueber refraktionsseismische Messungen in Cumaná zur Bestimmung der seismischen Geschwindigkeiten. Unpublished Report, FUNVISIS, Caracas. 22 pp.

Lang, D.H., Raschke, M., Schwarz, J., 1999. The Cariaco, Venezuela, Earthquake of July 09, 1997: aftershock measurements, macroseismic investigations and engineering analysis of structural damage. VI Congreso Venezolano de Sismología e Ingeniería Sísmica, Mérida, Venezuela (CD-Rom format), 12 pp.

Masaki, K., Saguchi, K., Sánchez, A., 1998. On the 1997 Cariaco earthquake and microtremor observation in the Cariaco city. Taller sobre Microzonificación Sísmica en Países Vulnerables, Yokohama, Japón, 9–10 de marzo de 1998, Proceedings. 10 pp.

Mendoza, C., 2000. Rupture history of the 1997 Cariaco, Venezuela, earthquake from teleseismic P waves. Geophysical Research Letters 27, 1555–1558.

Metz, H.L., 1968. Stratigraphic and geologic history of extreme northeastern Serranía del Interior, State of Sucre, Venezuela. Fourth Caribbean Geological Conference, Port of Spain, Trinidad and Tobago, 1965. Transactions, Caribbean Printers, Arima, Trinidad and Tobago, pp. 275–292.

Minster, B.J., Jordan, T.H., 1978. Present-day plate motions. Journal of Geophysical Research 83, 5331–5354.

Mocquet, A., Contreras, R., 1999. Estudio macrosísmico del sismo de Cariaco. VI Congreso Venezolano de Sismología e Ingeniería Sísmica, Mérida, 12–14 de Mayo de 1999. 15 pp.

Mocquet, A., Beltrán, C., Lugo, M., Rodríguez, J.A., Singer, A., 1996. Seismological interpretation of the historical data related to the 1929 Cumaná earthquake, Venezuela. 3rd International Symposium on Andean Geodynamics. Editions de l' ORSTOM, Paris, pp. 203–206.

MTC, 1997. Daños de consideración causados en la vialidad principal del estado Sucre, como consecuencia del movimiento sísmico del día 09-07-97. Ministerio de Transporte y Comunicaciones-MTC-'s unpublished report.

Nakamura, Y., 1989. A method for dynamic characteristics estimation of subsurface using microtremor on the ground surface. QR of RTRI 30 (1), 25–33.

Palmer, D., 1986. Refraction Seismics. Seismic Exploration, vol. 13. Geophysical Press, London.

Rosenblueth, E., Ovando, E., 1991. Geotechnical lessons learned from Mexico and other recent earthquakes (state of the art paper). Proc. 2nd Int. Conf. on Recent Advances in Geotechnical Earthquake Engineering and Soil Dynamics, St. Louis, Missouri.

Sandmeier, K.J., 1998. REFRA—Program for Processing and Interpretation of Refraction seismic Data, Version 2, Karlsruhe, Germany. 168 pp.

Schmitz, M., Alvarado, L., Lüth, S., 2001. The velocity structure of the Cariaco sedimentary basin, northeastern Venezuela, from shallow wide-angle seismic data (submitted).

Schnabel, P.B., Lysmer, J., Seed, H.B., 1972. SHAKE: a computer program for earthquake response analysis of horizontally layered sites. Report No. EERC 72-12, Univ. of California, Berkeley.

Schwarz, J., Lang, D., Habenberger, J., Raschke, M., Baumbach, M., Grosser, H., Sobiesiak, M., Welle, W., Bonato, M.A., Hernández, A., Romero, G., Schmitz, M., Avendaño, J., 1998. The Cariaco, Venezuela, Earthquake of July 09, 1997: engineering analysis of structural damage. 11th European Conference on Earthquake Engineering, Paris. 12 pp.

Seed, H.B., Idriss, I.M., 1970. Soil moduli and damping factors for dynamic response analyses. EERC-Report 70-10, Berkeley, California.

Seed, H.B., Idriss, I.M., 1971. Simplified procedure for evaluating soil liquefaction potential. Journal of the Soil Mechanics and Foundations Division, ASCE 97, 1249–1273.

Seed, H.B., Idriss, I.M., Dezfulian, H., 1970. Relationships between soil conditions and building damage in the Caracas earthquake of July 29, 1967. EERC-Report 70-2, Berkeley, California. 40 pp.

Seed, H.B., Dickenson, S.E., Riemer, M.F., Bray, J.D., Sitar, N., Mitchell, J.K., Idriss, I.M., Kayen, R.E., Kropp, A., Harder Jr., L.F., Power, M.S., 1990. Preliminary report of the principal geotechnical aspects of the October 17, 1989 Loma Prieta earthquake, Earthquake Engineering Research Center, Report No. UCB/EERC-90-05. 137 pp.

Sheriff, R.E., Geldart, L.P., 1995. Exploration Seismology, 2nd ed. Cambridge Univ. Press, Cambridge, USA. 592 pp.

Sun, J.I., Golesorkhi, R., Seed, H.B., 1988. Dynamic moduli and damping ratios for cohesive soils. Report No. EERC-88/15, Univ. of California, Berkeley.

Vignali, M., 1979. Estratigrafía y estructura de las cordilleras metamórficas de Venezuela Oriental (Peninsula de Araya-Paria e Isla de Margarita). Escuela de Geología y Minería, UCV, Caracas. GEOS 25, 19–66.

Vucetic, M., Dobry, R., 1991. Effect of soil plasticity on cyclic response. Journal of Geotechnical Engineering, ASCE 117, 89–107.